iScience

CellPress
OPEN ACCESS

Article

AIBP protects drug-induced liver injury by inhibiting MAPK-mediated NR4A1 expression

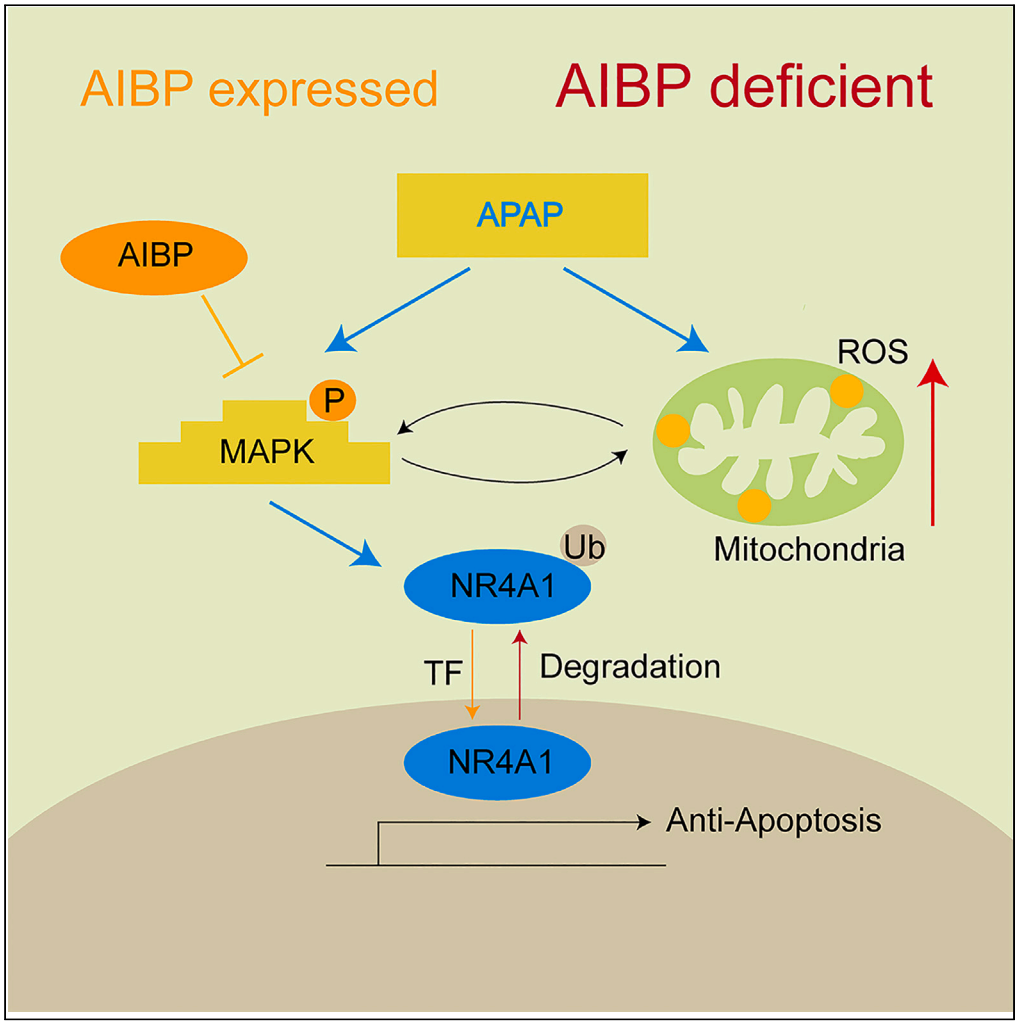

Tao Ma, Wei Huang, Yihong Ding, ..., Yihui Fan, Renfang Mao, Cuihua Lu

fanyihui@ntu.edu.cn (Y.F.)
maorenfang@ntu.edu.cn (R.M.)
lch670608@sina.com (C.L.)

Highlights

AIBP enhances NR4A1 expression and protects cells via NR4A1 under injury

AIBP protects liver injury by inhibiting MAPK signaling pathway

AIBP reduces mitochondrial stress and protects mitochondrial function

Ma et al., iScience 27, 110873
October 18, 2024
https://doi.org/10.1016/j.isci.2024.110873

iScience

CellPress
OPEN ACCESS

Article

AIBP protects drug-induced liver injury by inhibiting MAPK-mediated NR4A1 expression

Tao Ma,[1,2,7] Wei Huang,[1,7] Yihong Ding,[1,3,7] Ran Ji,[4] Sijia Ge,[1,2] Qingqing Liu,[1,2] Yiheng Liu,[1,2] Jing Chen,[1,2] Yang Yan,[1,2] Shushu Lu,[1,2] Qiqi Ren,[1,2] Yihui Fan,[5,*] Renfang Mao,[6,*] and Cuihua Lu[1,8,*]

SUMMARY

Drug-induced liver injury (DILI) is an important adverse drug reaction that can lead to acute liver failure or even death in severe cases. AIBP is a binding protein of apolipoprotein AI involved in lipid metabolism and maintenance of oxidative respiration in mitochondria, but its role in DILI is unclear. By constructing AIBP knockout mice, overexpressing and knocking down AIBP in cell lines, we established animal and cell models of DILI. Using western blotting and real-time qPCR assay, we explored the influence of AIBP in activation of mitogen-activated protein kinases (MAPK) signal pathways and possible targets. AIBP was downregulated during hepatocyte injury. AIBP deficient mice develop severe liver injury and more sensitive to drug-induced cell death. Overexpression of AIBP protects cells under APAP treatment. Furthermore, AIBP inhibits the activation of MAPK pathways, through which AIBP regulates NR4A1. These results suggest that AIBP is expected to become a valuable biomarker and therapeutic target in liver injury.

INTRODUCTION

Acute liver injury represents a prevalent clinical condition where the liver undergoes significant functional impairment within a short duration.[1] This condition can be attributed to diverse factors, such as excessive drug intake, toxic exposure, immune stress, metabolic disorders, and more.[2] The liver plays a crucial role in maintaining metabolic homeostasis, being involved in protein, lipid, and glucose metabolism, as well as the synthesis of most plasma proteins. However, factors like improper drug use and severe infections can trigger inflammatory responses, oxidative stress, and mitochondrial dysfunction in the liver, resulting in protein misfolding and hepatocyte death.[3] Among the causes of acute liver injury, acetaminophen (APAP) is a prominent one, commonly used as an antipyretic and analgesic medication.[4] Excessive intake of APAP can lead to liver toxicity, making it a leading cause of acute liver failure in Western countries.[5] This occurs because APAP undergoes metabolism in the liver, producing a toxic metabolite called N-acetyl-*p*-benzoquinimide (NAPQI).[6] NAPQI depletes intracellular reduced glutathione (GSH), binds to proteins, and leads to mitochondrial dysfunction, oxidative stress, DNA damage, necrosis, and liver injury.[7,8] But the cellular protein involved in APAP toxicity are largely unexplored.

Apolipoprotein A-I binding protein (AIBP) is a lipid-associated protein that binds to HDL and facilitates the transfer of cholesterol from HDL to surrounding tissues.[9–11] This aids in removing excessive cholesterol from the bloodstream and transporting it back to the liver for metabolism and elimination.[12–14] On the other hand, AIBP was also an epimerase that can convert R-NADHX to biologically useful S-NADHX which participates in metabolite repair, one part of a set of dedicated systems used by cells to rescue damaged metabolites.[15,16] Therefore, it is also known as NAXE.[17] Additionally, AIBP plays a role in regulating certain cell signaling pathways, including Notch, mitogen-activated protein kinases (MAPKs) and NF-κB pathway, which is involved in processes such as cell proliferation, differentiation.[18–20] Recently, AIBP was reported to inhibit inflammation in adipocytes and macrophage by suppressing toll-like receptor 4 (TLR4)-mediated inflammatory signaling pathways.[21–23] However, whether AIBP contributes to liver injury and its underlying mechanism remains to be addressed.

The MAPK family plays a crucial role in transmitting signals from the cell surface to the nucleus, thereby regulating essential cellular processes such as cell proliferation, differentiation, stress response, and apoptosis.[24] Extensive research has demonstrated that the activation of MAPK is a critical event in liver injury and regeneration.[25] NR4A1(Nur77) is a member of the NR4A nuclear receptor family of intracellular transcription factors, and a downstream regulatory target of the MAPK family, involved in the regulation of proliferation, differentiation, inflammation, apoptosis, survival, and other cellular biological processes.[26,27] High level of NR4A1 can inhibit tumor cell apoptosis and promote cell proliferation.[28–30] Studies have suggested that NR4A1 can enhance the expression of anti-apoptotic proteins in pancreatic β cells, inhibit

[1]Department of Gastroenterology, Affiliated Hospital of Nantong University, Medical School of Nantong University, Nantong 226001, China
[2]Research Center of Clinical Medicine, Nantong University, Affiliated Hospital of Nantong University, Nantong, China
[3]Department of Gastroenterology, Rugao People's Hospital, Nantong, Jiangsu, China
[4]Department of Gastroenterology, Nantong First People's Hospital, Nantong, Jiangsu, China
[5]Department of Pathogenic Biology, School of Medicine, Nantong University, Nantong, Jiangsu, China
[6]Department of Pathophysiology, School of Medicine, Nantong University, Nantong, Jiangsu, China
[7]These authors contributed equally
[8]Lead contact
*Correspondence: fanyihui@ntu.edu.cn (Y.F.), maorenfang@ntu.edu.cn (R.M.), lch670608@sina.com (C.L.)
https://doi.org/10.1016/j.isci.2024.110873

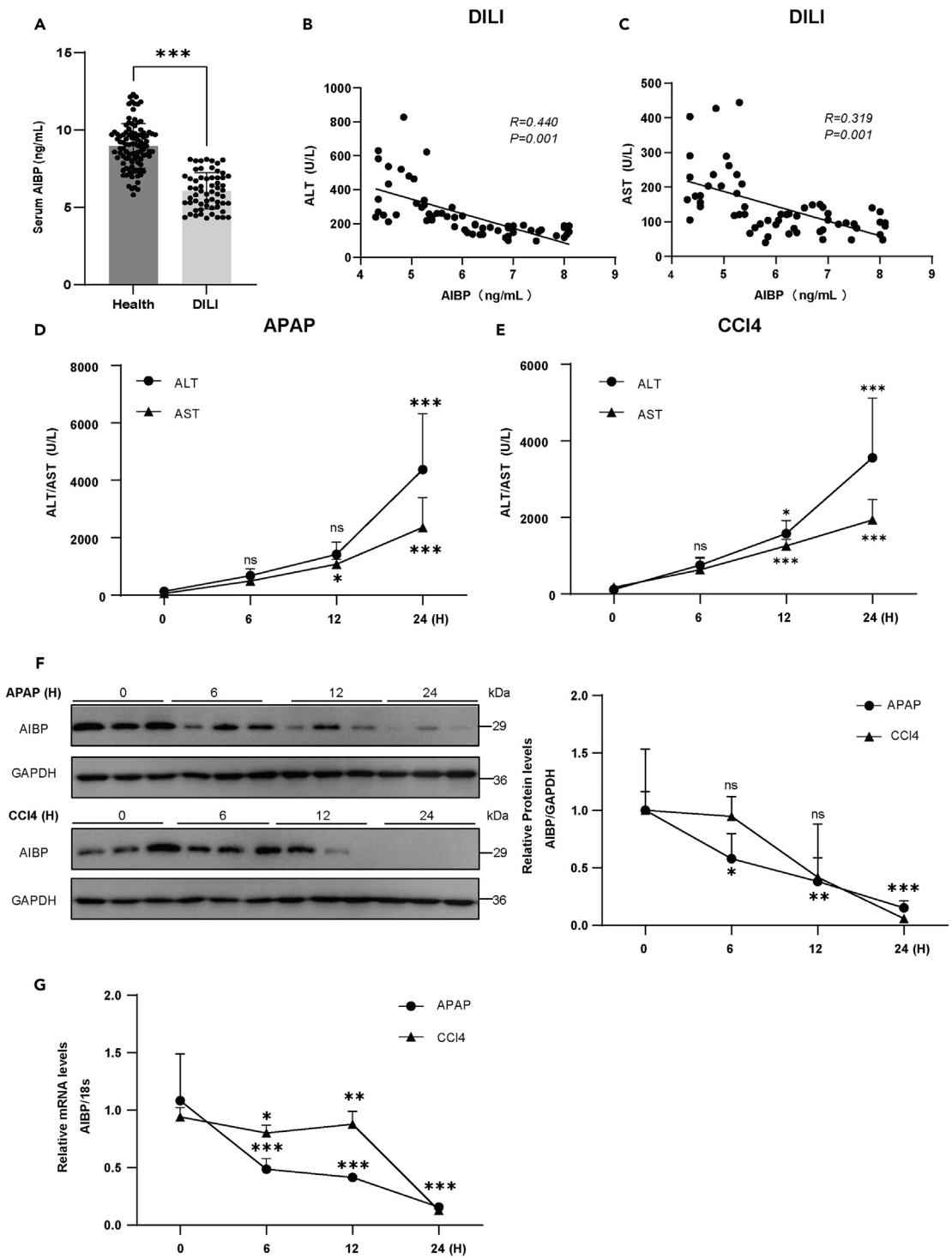

Figure 1. Downregulation of AIBP upon liver injury in multiple conditions

(A) Serum AIBP protein levels were detected by ELISA in 60 healthy subjects and 101 patients with acute liver injury.

(B and C) Correlation between liver injury parameters and serum AIBP expression (Pearson correlation test was used).

(D) Serum alanine aminotransferase and aspartate aminotransferase levels of wild-type (WT) C57BL6J mice treated with APAP for 6,12,24 h (N = 5).

(E) Serum alanine aminotransferase and aspartate aminotransferase levels in WT mice treated with CCl4 (N = 5).

(F) Western blotting was performed to detect AIBP protein levels in the livers of three APAP-treated mice (*top*) and three random CCl4-treated mice (*bottom*).

(G) The real-time qPCR analysis of AIBP mRNA levels in the liver of APAP-treated mice and CCl4-treated mice.

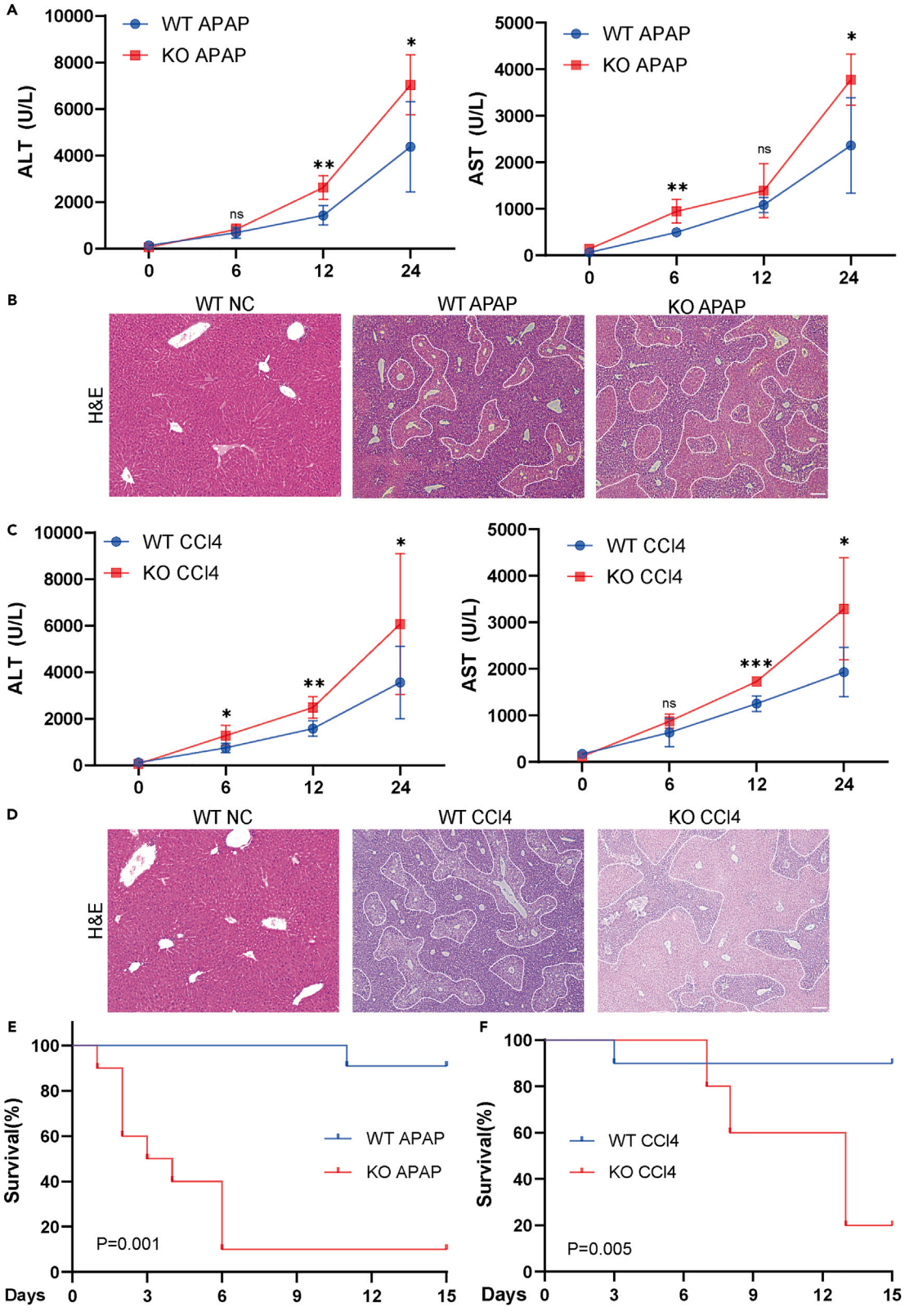
A
ALT (U/L)
WT APAP
KO APAP
ns
**
*
AST (U/L)
WT APAP
KO APAP
**
ns
*
B
WT NC
WT APAP
KO APAP
H&E
C
ALT (U/L)
WT CCl4
KO CCl4
*
**
*
AST (U/L)
WT CCl4
KO CCl4
ns
***
*
D
WT NC
WT CCl4
KO CCl4
H&E
E
Survival(%)
WT APAP
KO APAP
P=0.001
Days
F
Survival(%)
WT CCl4
KO CCl4
P=0.005
Days

Figure 2. AIBP deficient mice develop severe liver injury under multiple conditions

(A) Serum alanine aminotransferase and aspartate aminotransferase levels of WT and AIBP knockout (KO) C57BL6J mice treated with APAP for 6,12, and 24 h.

(B) H&E staining of WT and KO C57BL6J mice treated with APAP for 24 h (Scale bar: 200um).

(C) Serum alanine aminotransferase and aspartate aminotransferase levels in WT and KO C57BL6J mice treated with CCl4 for 6, 12 and 24 h.

(D) H&E staining of WT and KO C57BL6J mice treated with CCl4 for 24 h (Scale bar: 200um).

(E) Survival of WT and *AIBP* KO mice treated with APAP ($N = 10$).

(F) Survival of WT and *AIBP* KO mice treated with CCl4 ($N = 10$).

endoplasmic reticulum stress and reactive oxygen species (ROS) generation.[31] However, the relationship between AIBP and NR4A1 is unknown. Furthermore, how AIBP and NR4A1 regulate liver injury is also unclear.

In the current paper, we explored the role of AIBP in liver injury both *in vivo* and *in vitro*. We found that AIBP was downregulated in liver injury. Mechanistically, in acute liver injury, AIBP inhibited the activation of MAPKs and upregulated the expression of NR4A1, probably via the ubiquitination pathway. These findings indicate that AIBP is a valuable biomarker and therapeutic target of liver injury.

RESULTS

AIBP is downregulated in human serum and animal DILI livers

To explore the expression of AIBP in drug-induced liver injury (DILI), we first detected the levels of AIBP in serum samples of 60 patients with DILI and 101 healthy people by ELISA assay. As shown in Figure 1A, the expression of AIBP was significantly lower in DILI patients than that in healthy people. Correlation analysis showed that the levels of AIBP was negatively correlated with ALT and AST in DILI patients (Figures 1B and 1C), suggesting that AIBP may play an important role in DILI. Thus, we constructed an DILI model in C67BL/6J mice by intraperitoneal injection of APAP and CCl4 to detect the expression of AIBP, and found that the serum levels of ALT and AST activities increased gradually in a time-dependent manner after APAP and CCl4 injection (Figures 1D and 1E). Similarly, following APAP and CCl4 injection, the protein and mRNA levels of AIBP decreased gradually with the prolongation APAP and CCl4 injection time (Figures 1F and 1G). These results suggested that AIBP was downregulated in DILI and might play an important role in the development of DILI.

AIBP deficiency aggravated DILI induced by APAP and CCl4

In order to better understand the role of AIBP in the development of DILI, mouse strains with knockout of AIBP (KO) were constructed by CRISPR/Cas9-mediated genome engineering. By intraperitoneal injection of APAP and CCl4, we found that compared with WT mice, AIBP KO mice showed higher serum ALT and AST levels (Figures 2A and 2C). H&E staining further demonstrated severe liver damage in AIBP KO mice than that in WT mice (Figures 2B and 2D). In addition, by monitoring the survival time of mice after APAP and CCl4 injection, we found that compared with WT mice, knockout of AIBP gene significantly reduced the survival time of mice (Figures 2E and 2F). Taken together, our results indicated that knockout of AIBP could exacerbate hepatocytes injury induced by APAP and CCl4, resulting in more severe liver function damage and reduced survival time of mice.

Downregulation of AIBP increased cells sensitivity to APAP-induced injury *in vitro*

To explore the protective role of AIBP in cell injury induced by APAP *in vitro*, we first detected the expression of AIBP in HepG2, SMMC-7721, and LO2 cells with or without APAP stimulation, and found that with the increase of APAP does, the expression of AIBP was significantly decreased both in protein and mRNA levels (Figures S1A–S1C). However, we found that the proportion of dead cells in LO2 cells treated with 20mM APAP was significantly higher than that in HepG2 and SMMC-7721 (Figure S1D), suggesting that LO2 cells were less tolerant to APAP-induced cell injury. Thus, we established a stable AIBP knockdown cell line in SMM-7721 cells and a stable AIBP overexpression cell line in HepG2 cells (Figures S1E and S1F).

Next, we further determined the effect of AIBP on APAP-induced cell injury. Propidium iodide (PI) staining results shown that compared with the control group (sgVEC+NC), APAP stimulation (sgVEC+APAP) could induce cell death, and found that knockdown AIBP could significantly increase the proportion of cell death induced by APAP (Figure 3A). The flow cytometry further validated that downregulation of AIBP could increase the percentage of apoptotic cells induced by APAP treatment (Figure 3B). In addition, trypan blue staining and CCK8 assay also shown that downregulation of AIBP could significantly promote cell death and reduce cell viability (Figures 3C and 3D), and the number of adherent cells was significantly reduced in AIBP knockdown group than that in control group (Figure 3E). Finally, western blotting results revealed that knockdown AIBP could enhance the bax activation and caspase3 cleavage, as well as increased the expression of RIP3 and the phosphorylation of MLKL induced by APAP (Figures 3F and 3G). However, the results of overexpression of AIBP in HepG2 cells were reverse (Figure 4). These results suggested that ectopic expression of AIBP could regulate the sensitivity of cells to APAP.

Overexpression of NR4A1 ameliorated cells injury induced by APAP

In order to further explore the mechanism of AIBP protection against DILI, we examined the expression of several downstream targets of AIBP, and found that overexpression of AIBP greatly increased the expression of NR4A1 in HepG2 cells (Figure 5A). Consistently, downexpression of AIBP also reduced the expression of NR4A1 in SMM-7721 cells (Figure 5B). However, the mRNA level of NR4A1 upon overexpression or downexpression of AIBP was minorly changed (Figures 5C and 5D), indicating AIBP might regulate NR4A1 expression post-translationally. Previous studies had shown that NR4A1 is a key gene for cell survival under stress,[32,33] thus we speculated whether NR4A1 is involved

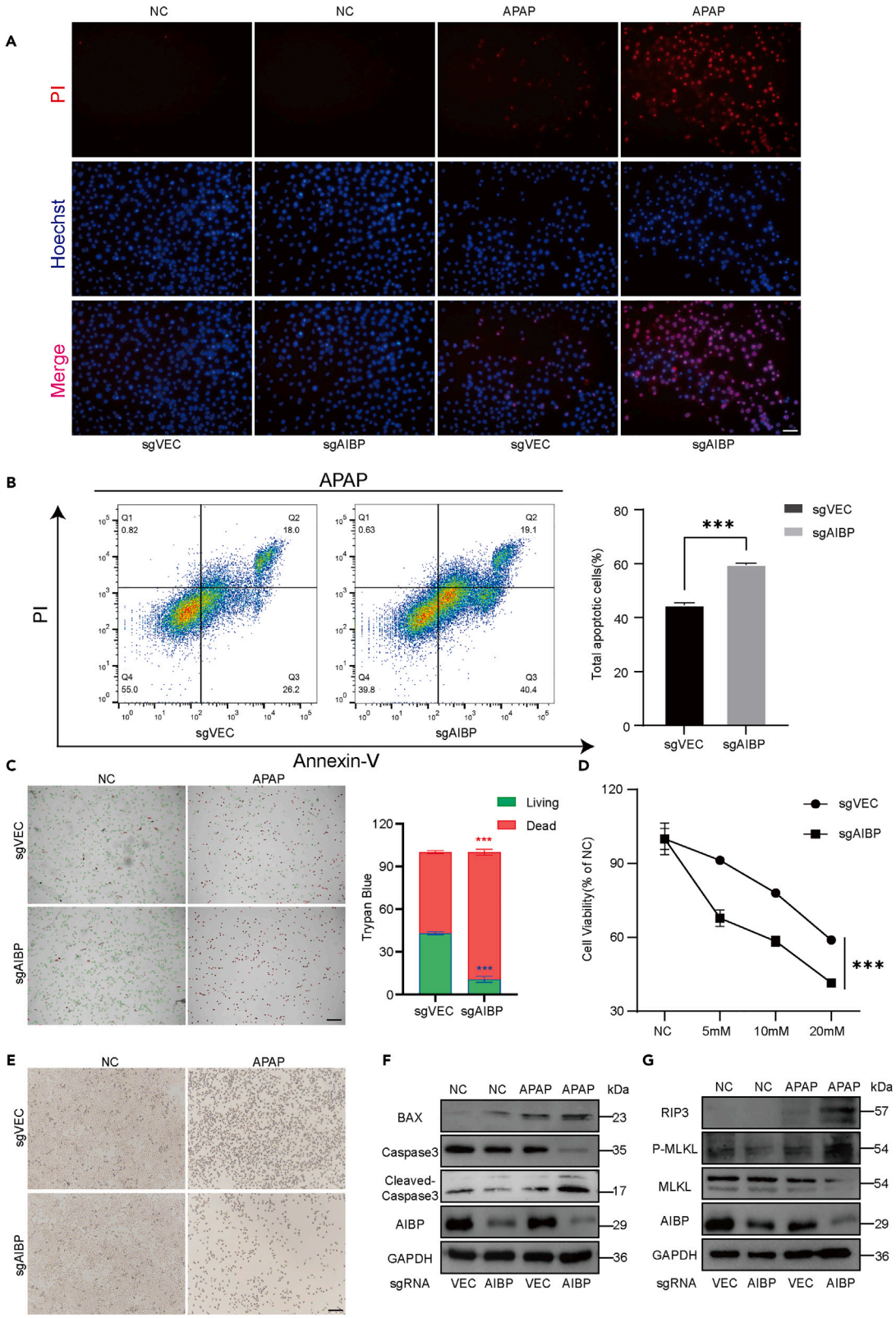
A
NC
NC
APAP
APAP
PI
Hoechst
Merge
sgVEC
sgAIBP
sgVEC
sgAIBP
B
APAP
PI
Annexin-V
Q1
0.82
Q2
18.0
Q4
55.0
Q3
26.2
Q1
0.63
Q2
19.1
Q4
39.8
Q3
40.4
sgVEC
sgAIBP
Total apoptotic cells(%)
***
sgVEC
sgAIBP
C
NC
APAP
sgVEC
sgAIBP
Living
Dead
Trypan Blue
***
***
sgVEC
sgAIBP
D
Cell Viability(% of NC)
sgVEC
sgAIBP
***
NC
5mM
10mM
20mM
E
NC
APAP
sgVEC
sgAIBP
F
NC
NC
APAP
APAP
kDa
BAX
Caspase3
Cleaved-Caspase3
AIBP
GAPDH
23
35
17
29
36
sgRNA
VEC
AIBP
VEC
AIBP
G
NC
NC
APAP
APAP
kDa
RIP3
P-MLKL
MLKL
AIBP
GAPDH
57
54
54
29
36
sgRNA
VEC
AIBP
VEC
AIBP

Figure 3. AIBP deficient cells are sensitive to injury *in vitro*

(A–C) 7721 control and AIBP knockdown cell lines were treated with 10mM APAP for 24 h to detect cell death. (A) PI staining (*red*) to detect necrotic cells (Scale bar: 100um). PI, propyl iodide. (B) Flow cytometry was used to detect apoptotic cells. The sum of Annexin-V single positive early apoptotic cells and Annexin-V and PI double-positive late apoptotic or necrotic cells was the total apoptotic cells. (C) Trypan Blue staining was used to detect cell mortality, and C100 automatic counter was used to label dead cells (Scale bar: 100um).

(D) The 7721 control and AIBP knockdown cells were treated with different doses of APAP (0, 5, 10, 20mM) for 24 h, and the cell viability was detected by CCK8.

(E) 24 h after APAP treatment of 7721 control and AIBP knockdown cells, microscopic images of residual cells were taken (Scale bar: 100um).

(F and G) The protein expressions of apoptosis markers BAX, Caspase3, Cleaved Caspase3, and necrosis markers RIP3, P-MLKL, and MLKL were detected by western blotting after 24 h of the 7721 control and AIBP knockdown cells treated with APAP.

in the cell injury process regulated by AIBP. Interestingly, immunofluorescence co-localization assay results showed that AIBP and NR4A1 proteins were co-localized in cytoplasm in SMM-7721 cells (Figure 5E). Furthermore, coimmunoprecipitation (coIP) assay result showed that AIBP interacts with NR4A1 in SMM-7721 cells (Figure 5F). These results suggested that AIBP may regulate the expression of its downstream gene NR4A1 through post-translational modification.

To evaluate the potential effects of NR4A1 in cell injury regulated by AIBP, we up-expressed the expression of NR4A1 in HepG2 cells. PI staining, trypan blue staining and CCK8 assay results shown that overexpression of NR4A1 also could significantly protect cell death and increase cell viability (Figures 6A–6C), and the number of adherent cells was significantly increased in NR4A1 overexpression group than that in control group (Figure 6D). Finally, western blotting results revealed that overexpression of NR4A1 could alleviate the bax activation and caspase3 cleavage, as well as reduce the expression of RIP3 and the phosphorylation of MLKL induced by APAP (Figures 6E and 6F). These results suggested that overexpression of NR4A1 could ameliorate cells injury induced by APAP.

NR4A1 largely restore cell injury in the case of down-regulated AIBP

To further explore the relationship between NR4A1 and AIBP in cell injury, we constructed a stable cell line with overexpression of NR4A1 in AIBP downregulated cells. PI staining results shown that compared with the control group (sgAIBP+VEC+APAP), overexpression of NR4A1 could significantly reduce the proportion of cell death in the case of downregulated AIBP (Figure 7A). Consistently, the percentage of apoptotic cells was significantly reduced upon overexpression of NR4A1 in AIBP downregulated group (Figure 7B). In addition, trypan blue staining and CCK8 assay further validated the partial rescue of cell injury caused by NR4A1 upregulated in the case of downregulated AIBP (Figures 7C and 7D), and the remaining cells in NR4A1 upregulated group were increased (Figure 7E). Finally, the level of cleaved caspase-3, Bax, RIP3, and *p*-MLKL was also partially restored in NR4A1 upregulated group (Figure 7F). In addition, by tail intravenous Nr4a1 overexpressed AAV9, we found that Nr4a1 can partially restore by AIBP defects caused liver damage degree added (Figures S2A and S2B). Taken together, these results suggested that overexpression of NR4A1 could partially reverse the cell damage caused by downregulation of AIBP.

AIBP protects liver injury by inhibiting MAPK signaling pathway

Previous studies have shown that AIBP could inhibit the activation of MAPK signaling pathway.[20] In cell injury, we also determined the effect of AIBP on MAPK signaling pathway. We first examined the protein and phosphorylation levels of genes associated with the MAPK signaling pathway in cell injury induced by APAP at different doses. The results shown that the phosphorylation levels of ERK, p38 and JNK increased gradually in the presence of increased concentration of APAP (Figures 8A and 8B). Interestingly, we found that the phosphorylation of ERK, P38, and JNK was reduced upon AIBP overexpression (Figures 8C and 8D). Conversely, the level of phosphorylation of ERK, P38, and JNK was increased upon AIBP knockdown (Figures 8C and 8D). In addition, we examined the level of phosphorylation of ERK, P38, and JNK in DILI model mouse liver tissue. Consistently, the level of phosphorylation of ERK, P38, and JNK was increased in AIBP deficient mice (Figures 8E and 8F). Next, we wonder whether inhibition of ERK, P38, and JNK activation could block APAP-induced NR4A1 downregulation. HepG2 and SMMC-7721 cells were treated with ERK inhibitor GDC-0994, p38 inhibitor SB203580 and JNK inhibitor SP 600125, and we found that inhibition of P38, JNK, and ERK activation greatly block APAP-induced downregulation of NR4A1 (Figures 8G and 8H). Furthermore, inhibition of P38, JNK, and ERK activation also partially block NR4A1 downregulation in the case of downregulated AIBP (Figures 8I and 8J). These results demonstrated that AIBP protects liver injury may be through inhibiting the activation of MAPK signaling pathway.

In order to further explore whether regulates NR4A1 through MAPK signaling pathway, we examined the expression and localization of NR4A1 in response to cell injury. As shown in Figure 5C, immunofluorescence assays shown that the expression of NR4A1 is not only present in the cytoplasm, but also expressed in the nucleus. And this was also confirmed by the nuclear/plasm separation assays (Figure S3A). Interestingly, we found that the expression of NR4A1 in the nucleus was reduced in HepG2 cells stimulated with APAP and was increased in the case of AIBP overexpression (Figures S3A and S3C). However, the mRNA level of NR4A1 was upregulated in response to cell injury induced by APAP, but was decreased upon overexpressing AIBP (Figure S3B). This opposite result suggested that AIBP may regulate NR4A1 expression through protein post-translational modification. As ubiquitination is the most common protein degradation pathway, MG132 was used to inhibit ubiquitin degradation. In this study, we found that the expression of NR4A1 and ubiquitin was increased in MG132-treated HepG2 cells (Figure S3D). These results indicate that NR4A1 is a protein that is degraded by ubiquitination. Next, we tested whether inhibition of MAPK activation could block APAP-induced NR4A1 downregulation by ubiquitination. We found that inhibition of MAPK activation suppressed APAP-induced downregulation of NR4A1 by inhibiting Ub generation (Figure S3E).

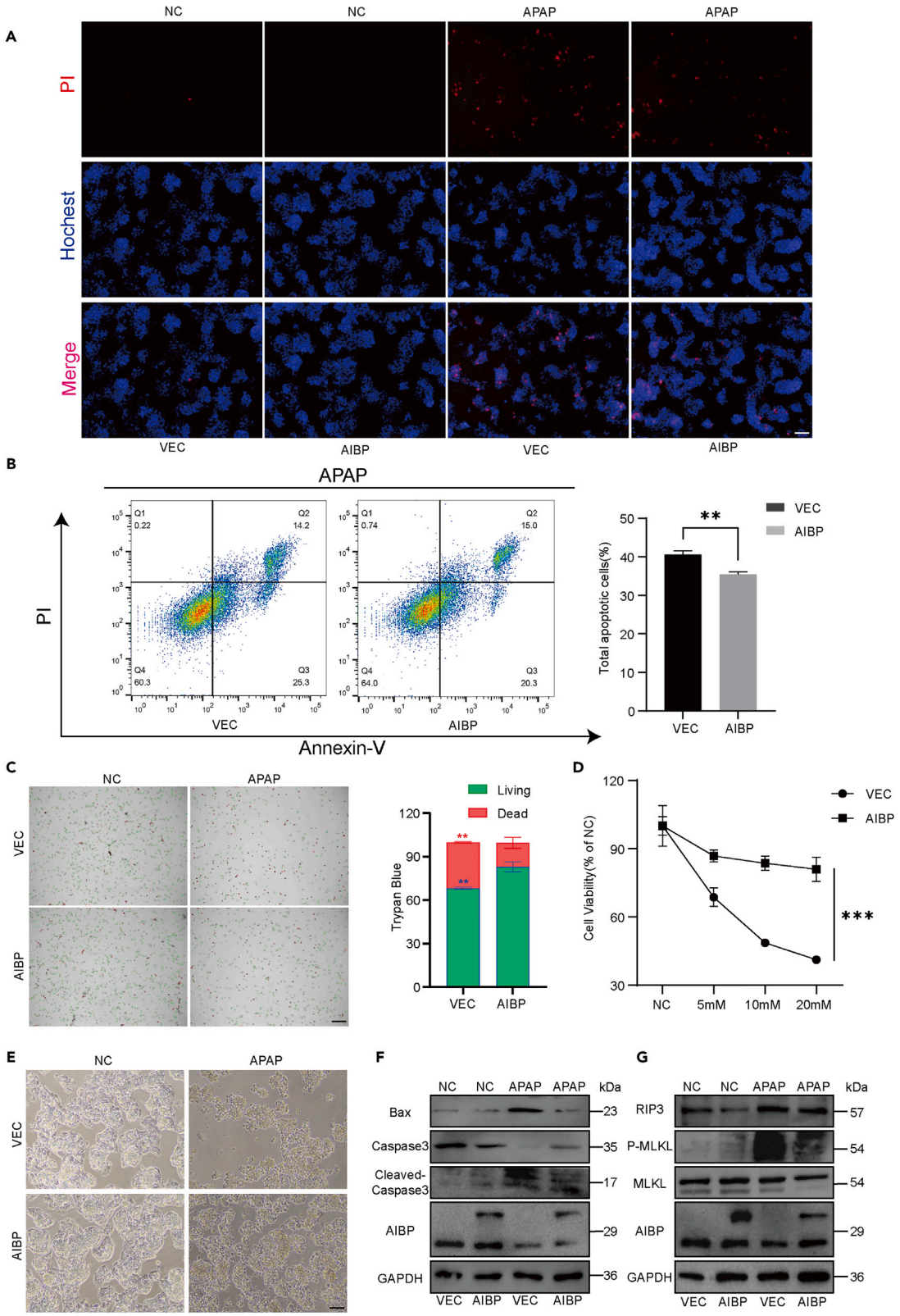
A
NC
NC
APAP
APAP
PI
Hochest
Merge
VEC
AIBP
VEC
AIBP
B
APAP
PI
Annexin-V
Q1 0.22
Q2 14.2
Q4 60.3
Q3 25.3
Q1 0.74
Q2 15.0
Q4 64.0
Q3 20.3
VEC
AIBP
Total apoptotic cells(%)
**
VEC
AIBP
C
NC
APAP
VEC
AIBP
Living
Dead
Trypan Blue
**
**
VEC
AIBP
D
Cell Viability(% of NC)
VEC
AIBP
***
NC
5mM
10mM
20mM
E
NC
APAP
VEC
AIBP
F
NC NC APAP APAP kDa
Bax
Caspase3
Cleaved-Caspase3
AIBP
GAPDH
23
35
17
29
36
VEC AIBP VEC AIBP
G
NC NC APAP APAP kDa
RIP3
P-MLKL
MLKL
AIBP
GAPDH
57
54
54
29
36
VEC AIBP VEC AIBP

Figure 4. *In vitro* overexpression of AIBP protects against drug-induced acute liver injury

(A–C) HepG2 control and AIBP overexpressed cell lines were treated with 10mM APAP for 24 h to detect cell death.

(A) PI staining (*red*) to detect necrotic cells (Scale bar: 100um). PI, propyl iodide.

(B) Flow cytometry was used to detect apoptotic cells. The sum of Annexin-V single positive early apoptotic cells and Annexin-V and PI double-positive late apoptotic or necrotic cells was the total apoptotic cells.

(C) Trypan Blue staining was used to detect cell mortality, and C100 automatic counter was used to label dead cells (Scale bar: 100um).

(D) HepG2 control cells and AIBP overexpressed cells were treated with different doses of APAP (0, 5, 10, 20mM) for 24 h, and cell viability was detected by CCK8.

(E) 24 h after APAP treatment of HepG2 control and AIBP overexpressed cells, microscopic images of residual cells were taken (Scale bar: 100um).

(F and G) Protein expressions of apoptosis markers BAX, Caspase3 and Cleaved Caspase3 and necrosis markers RIP3, P-MLKL and MLKL were detected by western blotting 24 h after APAP treatment of HepG2 control and AIBP overexpressed cells.

AIBP reduces mitochondrial stress and protects mitochondrial function

It has been reported that mitochondrial damage and oxidative stress induced by JNK phosphorylation and mitochondrial shift may be the core events of acute liver injury.[25,34,35] As shown in Figure 9A, AIBP exists in the cytoplasm of SMMC-771 cells. And we further confirmed that AIBP exists in the cytoplasm of SMMC-771 cells through nuclear/plasma separation assays (Figure 9B). NRF2 is the main transcription

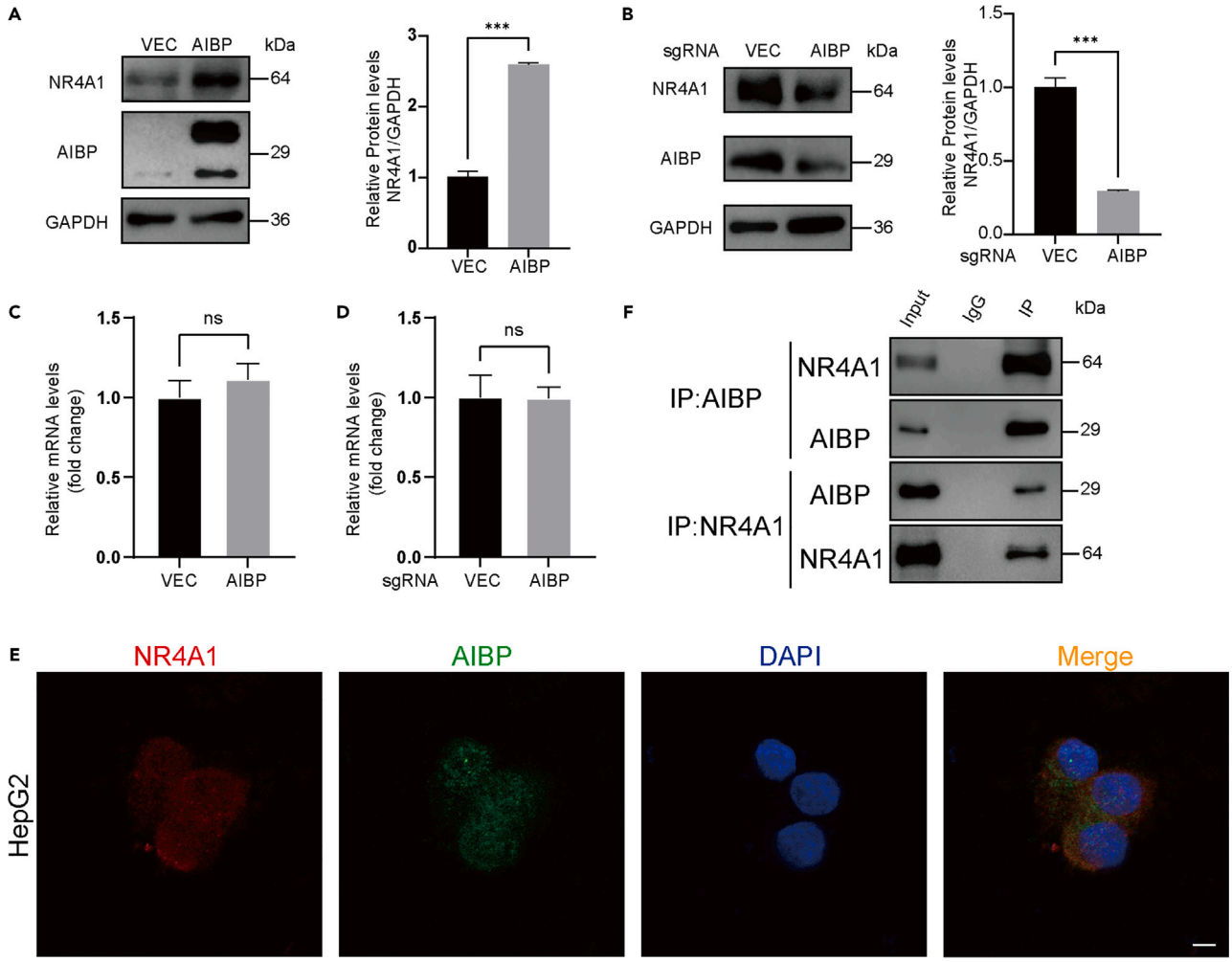

Figure 5. AIBP enhances the expression of NR4A1

(A) Western blotting was used to detect NR4A1 protein expression in HepG2 control and AIBP overexpressed cell lines.

(B) Western blotting was used to detect NR4A1 protein expression in control and AIBP knockdown cell lines 7721.

(C) Real-time qPCR was used to analyze NR4A1 mRNA expression levels in HepG2 control and AIBP overexpressed cell lines.

(D) Real-time qPCR was used to analyze the mRNA expression level of NR4A1 in control and AIBP knockdown cell lines 7721.

(E) Confocal immunofluorescence showed that AIBP(Green) and NR4A1(Red) were colocalized in the cell cytoplasm in HepG2 cells. Nuclei were stained with DAPI (Blue). Scale bar: 10um.

(F) Endogenous Co-IP assays were performed in HepG2 cells, IgG was used as control.

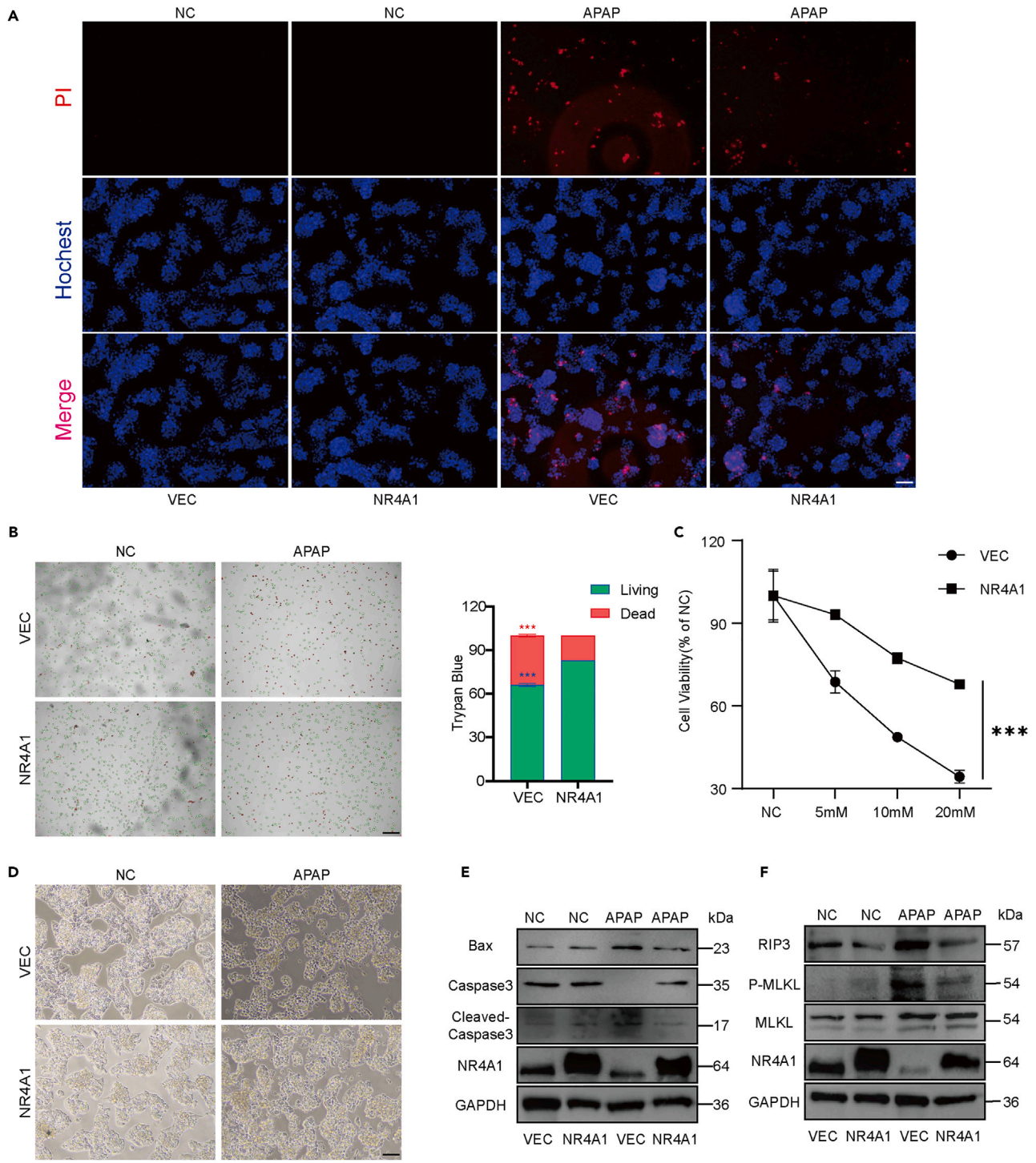

Figure 6. NR4A1 protects cellular liver damage induced by APAP

(A) PI staining (*red*) to detect necrotic cells (Scale bar: 100um). PI, propyl iodide.

(B) Trypan Blue staining was used to detect cell mortality, and C100 automatic counter was used to label dead cells (Scale bar: 100um).

(C) HepG2 control cells and NR4A1 overexpressed cells were treated with different doses of APAP (0, 5, 10, 20mM) for 24 h, and cell viability was detected by CCK8.

(D) 24 h after APAP treatment of HepG2 control and NR4A1 overexpressed cells, microscopic images of residual cells were taken (Scale bar: 100um).

(E and F) After APAP treatment of HepG2 control and NR4A1 overexpressed cells for 24 h, western blotting detected the protein expressions of apoptosis markers BAX, Caspase3, Cleaved Caspase3, and necrosis markers RIP3, P-MLKL, MLKL.

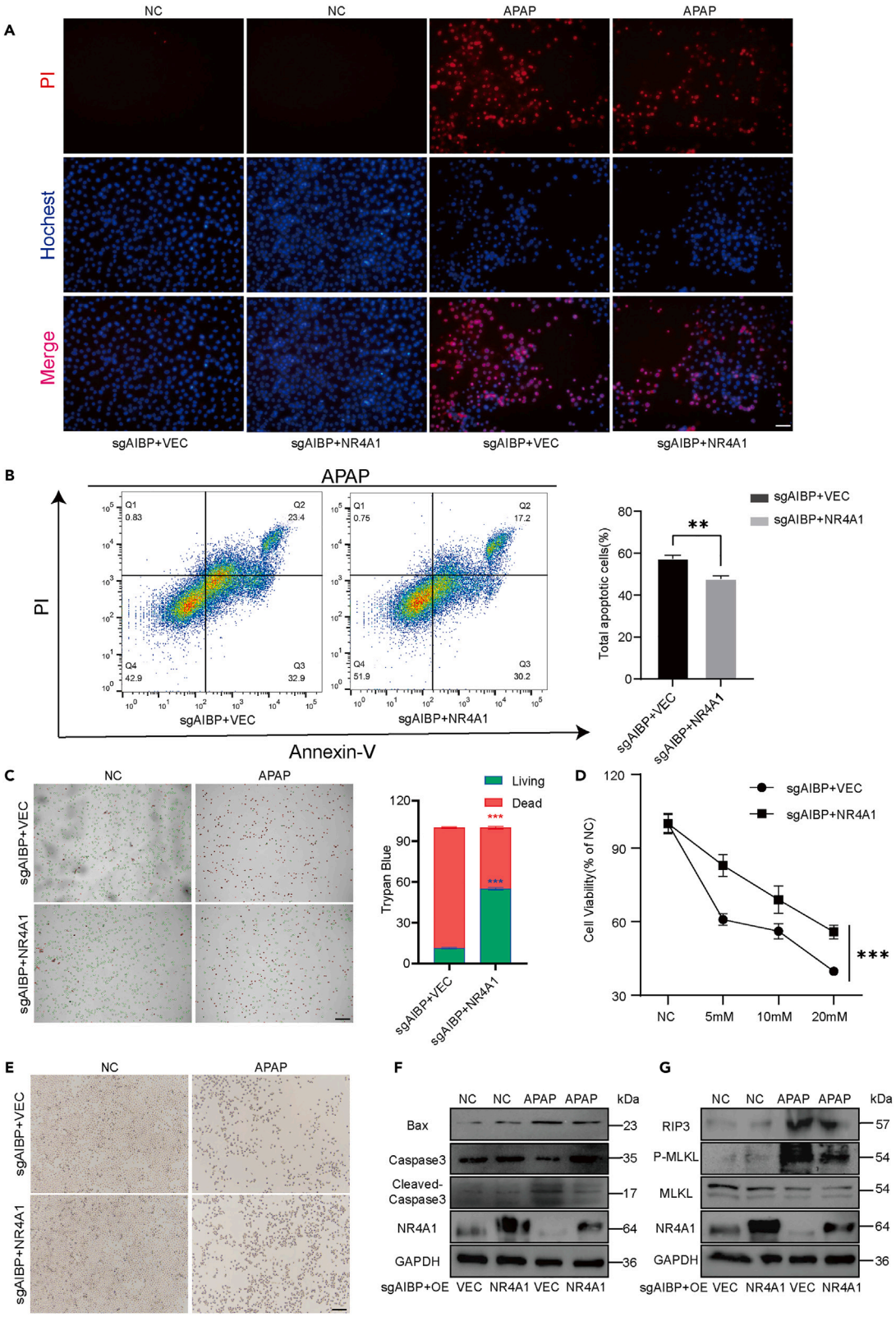
A
NC
NC
APAP
APAP
PI
Hochest
Merge
sgAIBP+VEC
sgAIBP+NR4A1
sgAIBP+VEC
sgAIBP+NR4A1
B
APAP
PI
Annexin-V
Q1 0.83
Q2 23.4
Q4 42.9
Q3 32.9
Q1 0.75
Q2 17.2
Q4 51.9
Q3 30.2
sgAIBP+VEC
sgAIBP+NR4A1
sgAIBP+VEC
sgAIBP+NR4A1
Total apoptotic cells(%)
**
C
NC
APAP
sgAIBP+VEC
sgAIBP+NR4A1
Living
Dead
***
***
Trypan Blue
sgAIBP+VEC
sgAIBP+NR4A1
D
sgAIBP+VEC
sgAIBP+NR4A1
Cell Viability(% of NC)
***
NC
5mM
10mM
20mM
E
NC
APAP
sgAIBP+VEC
sgAIBP+NR4A1
F
NC NC APAP APAP kDa
Bax 23
Caspase3 35
Cleaved-Caspase3 17
NR4A1 64
GAPDH 36
sgAIBP+OE VEC NR4A1 VEC NR4A1
G
NC NC APAP APAP kDa
RIP3 57
P-MLKL 54
MLKL 54
NR4A1 64
GAPDH 36
sgAIBP+OE VEC NR4A1 VEC NR4A1

Figure 7. NR4A1 can restore APAP-induced liver injury in the absence of AIBP

(A–C) 7721 knockdown AIBP cell line overexpressed control cells and NR4A1 cells were treated with 10mM APAP for 24 h to detect cell death.

(A) PI staining (*red*) to detect necrotic cells (Scale bar: 100um). PI, propyl iodide.

(B) Flow cytometry was used to detect apoptotic cells. The sum of Annexin-V single positive early apoptotic cells and Annexin-V and PI double-positive late apoptotic or necrotic cells was the total apoptotic cells.

(C) Trypan Blue staining was used to detect cell mortality, and C100 automatic counter was used to label dead cells (Scale bar: 100um).

(D) Overexpressed control and NR4A1 cells in 7721 knockdown AIBP cell lines were treated with different doses of APAP (0, 5, 10, 20mM) for 24 h, and cell viability was detected by CCK8.

(E) 24 h after APAP treatment of overexpressed control and NR4A1 cells from 7721 knockdown AIBP cell line, the residual cells were photographed by microscope (Scale bar: 100um).

(F and G) Protein expressions of apoptosis markers BAX, Caspase3, Cleaved Caspase3, and necrosis markers RIP3, P-MLKL, and MLKL were detected by western blotting after 24 h treatment with APAP in the overexpressed control and NR4A1 cells of the 7721 knockdown AIBP cell line.

factor that reflects the antioxidant level of cells, and can promote the expression of antioxidant genes.[36–38] In this study, we also detected the expression of NRF2 in HepG2 cells transfected with control or AIBP overexpression plasmid. The result shown that the expression of NRF2 was increased in AIBP-overexpressed cells, while reduced in injury cells induced by APAP (Figure 9C). In addition, we found that the downregulation of NRF2 induced by APAP was partially restored upon overexpression of AIBP (Figure 9C). Meanwhile, real-time qPCR assay also detected the high transcription levels of NRF2 downstream antioxidant target genes, including NQO1, GSTA3, and AKR1C in overexpression of AIBP cells (Figure 9D). Finally, we also detected the mitochondrial membrane potential in 7721 cells stimulated with APAP. As shown in Figure 9E, APAP could induce mitochondrial dysfunction (labeled by monomers of JC1 reagent), while was greatly reduced upon over-expression of AIBP. And found that the levels of ROS were increased upon APAP treatment, while were blocked by inhibitors of P38 and JNK (Figure 9F). Our results demonstrated that AIBP could stabilize mitochondrial oxidative respiration and protecting oxidative damage induced by APAP.

DISCUSSION

DILI is a clinical and pathological term that refers to liver injury caused by various drugs, leading to liver dysfunction.[1] The rapid progression of DILI is one of the main causes of acute liver failure, and severe patients require liver transplantation or even lead to death.[39,40] APAP excess is one of the main causes of DILI, with apoptosis and necrosis as the main pathways of hepatocyte death.[41] Therefore, revealing the underlying mechanisms of toxicity mediated by APAP is a key to overcoming liver injury. In this work, we have taken up the challenge of identifying AIBP perturbations in patients with DILI and investigated the effects by modulating AIBP in a preclinical DILI model. Our findings suggest that AIBP is a major mediator affecting liver injury. Because AIBP deficient mice show severe liver damage and much more sensitive to APAP-induced death. Furthermore, the level of AIBP was significantly downregulated upon liver injury. Thus, AIBP not only plays critical roles in liver injury, but also change significantly during the process. These results suggest a potential clinical application both as a biomarker or a therapeutic target in liver injury.

Oxidative stress and mitochondrial damage are the core events of DILI4. The hepatotoxic products of APAP or CCl4 bind to mitochondrial proteins, leading to inhibition of mitochondrial respiration and triggering mitochondrial damage and oxidative stress.[6] In response to oxidative stress, mitochondrial permeability changes occur, mitochondrial polarization, ATP production decreases, and free ROS increases.[42] Eventually, loss of mitochondrial membrane potential leads to swelling and rupture of the mitochondrial membrane and the release of the endonuclease. The endonuclease then translocates to the nucleus and cleaves nuclear DNA causing DNA damage. This eventually leads to cell necrosis.[4] Our results suggest that AIBP can reduce mitochondrial oxidative stress and protect mitochondrial function. Overexpression of AIBP promoted the expression of antioxidant gene NRF2 and the expression of corresponding downstream antioxidant target genes. AIBP maintains the stability of mitochondrial membrane potential during APAP liver injury. The relationship between AIBP and mitochondrial function is relevant to MAPK, as the use of MAPK inhibitors partially reduces the generation of free ROS.

Death of hepatocytes is the typical attribution of oxidative stress induced acute liver injury. APAP or CCl4 could induce a significant increase in hepatocyte death. In the present study, we found that APAP significantly increased the number of apoptotic and necrotic cells, while AIBP significantly reduced hepatocyte apoptosis and necrosis. Consistent with the reduction of apoptotic and necrotic cells, the expression of apoptosis-related protein Bax was downregulated, while the expression of necrosis-related protein RIP3 was downregulated in cells overexpressing AIBP. In addition to this, AIBP also improved the viability of APAP-poisoned cells and increased the number of surviving cells. In animal models, APAP or CCl4 overdose, gene deletion of AIBP significantly aggravated liver injury and promoted liver cell death. These results indicated that AIBP was the key gene against DILI. Hepatocyte death caused by APAP is closely related to cellular oxidative stress mainly caused by mitochondrial dysfunction. In the absence of AIBP, MAPK activation levels are elevated in favor of APAP-induced liver cell death, which is mainly due to mitochondrial ROS production and oxidative stress. These results suggest that AIBP can significantly ameliorate APAP or CCl4-induced liver injury by inhibiting oxidative stress-induced hepatocyte apoptosis and necrosis.

MAPK belong to a large family of serine-threonine kinases that form the major cellular signaling pathway from the cell surface to the nucleus. There are three major MAPK subfamilies (ERK, p38, and JNK) involved in the regulation of a variety of cell biological processes, including cell proliferation, apoptosis, and differentiation. Among them, ERK MAPK pathway has been proved to be one of the most important pathways in cell proliferation, which is involved in the maintenance of cell growth and differentiation. p38 and JNK may be associated with inflammation, apoptosis, and growth.[24] The interaction between JNK and mitochondria was crucial in promoting oxidative stress and

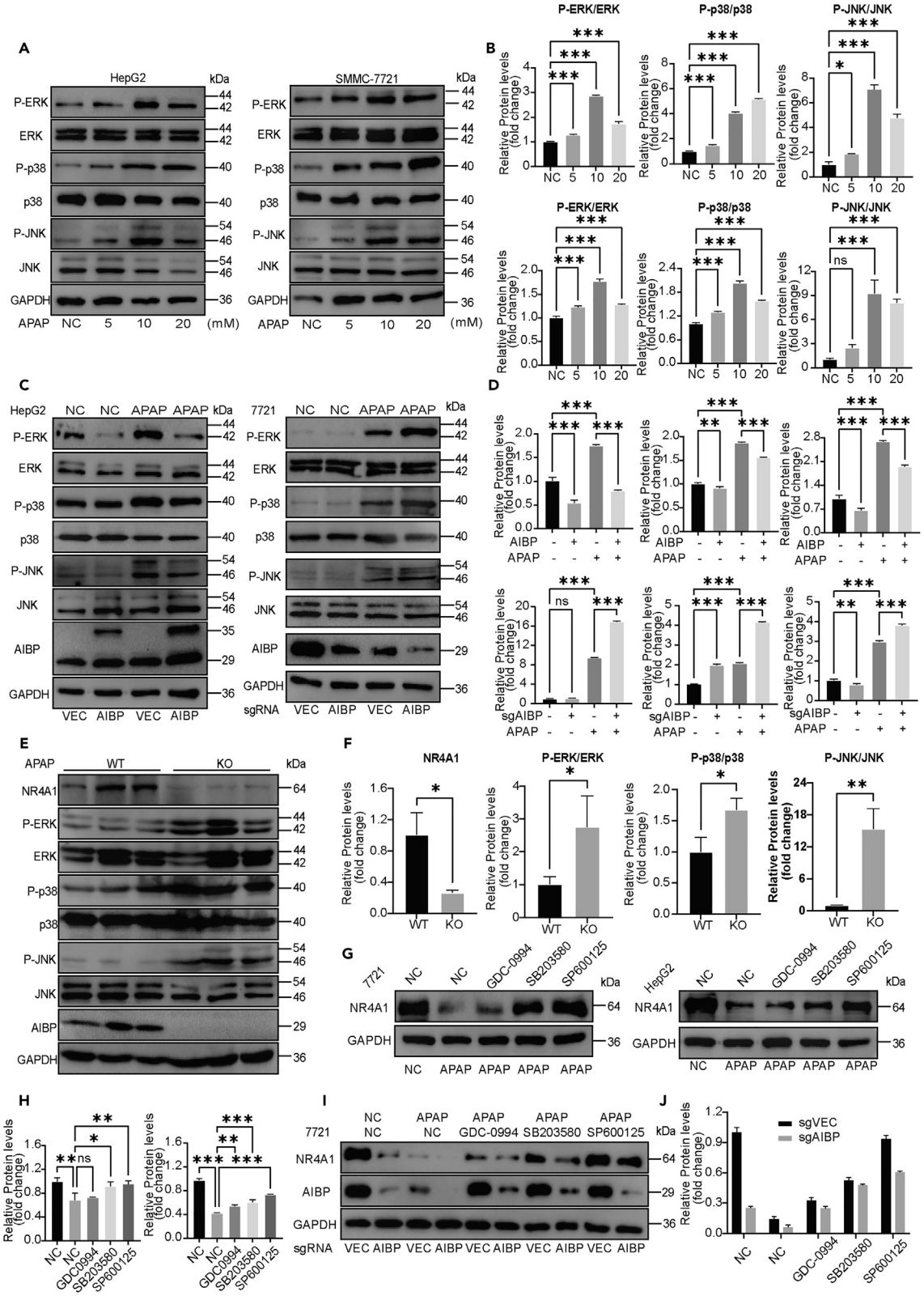
A
HepG2
kDa
P-ERK
ERK
P-p38
p38
P-JNK
JNK
GAPDH
APAP NC 5 10 20 (mM)
SMMC-7721
B
P-ERK/ERK
P-p38/p38
P-JNK/JNK
Relative Protein levels (fold change)
NC 5 10 20
C
HepG2 NC NC APAP APAP
7721 NC NC APAP APAP
AIBP
sgRNA
VEC AIBP VEC AIBP
D
AIBP
sgAIBP
APAP
E
APAP WT KO
NR4A1
F
NR4A1
WT KO
G
7721 NC NC GDC-0994 SB203580 SP600125
HepG2 NC NC GDC-0994 SB203580 SP600125
NC APAP APAP APAP APAP
H
NC NC GDC0994 SB203580 SP600125
I
NC NC APAP APAP APAP APAP
7721
GDC-0994 SB203580 SP600125
VEC AIBP VEC AIBP VEC AIBP VEC AIBP VEC AIBP
J
sgVEC
sgAIBP
NC NC GDC-0994 SB203580 SP600125

Figure 8. AIBP inhibits P-JNK and P-38 activation during liver injury

(A and B) HepG2 (*left, top*) and 7721 (*right, bottom*) cells were treated with different doses of APAP (0, 5, 10, 20mM), and the protein expressions of P-ERK, ERK, P-p38, p38, P-JNK, and JNK were detected by western blotting.

(C and D) APAP treated HepG2 overexpressing AIBP (*left, top*) and 7721 knockdown AIBP (*right, bottom*) cell lines, respectively, and western blotting detected the protein expressions of P-ERK, ERK, P-p38, p38, P-JNK and JNK.

(E and F) Protein expression of NR4A1, P-ERK, ERK, P-p38, p38, P-JNK and JNK in WT and *AIBP* KO mice treated with APAP were detected by western blotting.

(G and H) 7721 (*left*) and HepG2 (*right*) cells were pretreated with ERK inhibitor GDC-0994, p38 inhibitor SB 203580 and JNK inhibitor SP 600125 for 6 h, respectively, and then treated with APAP for 24 h. Western blotting was used to detect NR4A1 protein expression.

(I and J) Pretreatment 7721 control cells with ERK inhibitor GDC-0994, p38 inhibitor SB 203580 and JNK inhibitor SP 600125 were treated with AIBP knockdown cells for 6 h, and then treated with APAP for 24 h. Western blotting was used to detect the protein expression of NR4A1.

sustained JNK activation in the DILI study and is a central event in APAP-induced cell injury. APAP is metabolized by the liver to produce hepatotoxic active substance NQPQI.[6] The negatively charged NAPQI directly binds to mitochondrial proteins and initiates a self-amplified mitochondrial ROS → JNK → mitochondrial ROS cycle, which eventually leads to mitochondrial permeability changes and necrosis.[42] In the APAP model, multiple molecules are involved in the activation of JNK, which leads to mitochondrial outer membrane permeability and cell death.[41] In the present study, we confirmed that MAPK is activated in DILI. By using kinase inhibitors targeting MAPK, the inhibition of MAPK signaling partially restored the cellular ROS production induced by APAP, clarified its malignant role in the process of DILI, and identified the downstream target gene NR4A1 negatively regulated by MAPK signaling.

Nuclear receptor subfamily 4A group member 1 (NR4A1) belongs to the nuclear receptor superfamily and is an inducible multiple stress response factor.[26] The molecular structure of NR4A1 includes a transcriptional activation domain, a DNA-binding domain, and a ligand-binding domain, which can enhance the expression of some genes that are not ligand-bound.[26] NR4A1 regulates a wide range of biological processes, including apoptosis, autophagy, metabolism, inflammation, and survival.[43,44] However, the role of NR4A1 in apoptosis remains controversial. As a transcription factor, NR4A1 can enhance the expression of some anti-apoptotic factors.[45] NR4A1 can promote mitochondrial dysfunction leading to mitochondrial oxidative stress and apoptosis.[33] It is believed that the promoting or inhibiting effect of NR4A1 on apoptosis is related to its localization in cells. NR4A1 in the nucleus functions as a transcription factor to promote the transcription of anti-apoptotic genes, while NR4A1 in the cytoplasm induces mitochondrial damage and aggravates apoptosis, which may be related to the phosphorylation of NR4A1.[31] Numerous studies have shown that NR4A1 can be phosphorylated by upstream and downstream signaling molecules of the MAPK family, such as ERK, p38, and JNK.[46] Phosphorylated NR4A1 can induce apoptosis. Paradoxically, phosphorylation of NR4A1Ser351 by AKT inhibits its mitochondrial localization and proapoptotic activity.[47] Although our study suggests that NR4A1 plays a protective role in DILI against apoptosis, there are still many deficiencies in the understanding of its regulatory mechanism. We tend to think that NR4A1 has a protective role when it acts as a transcription factor, and that MAPK can downregulate the protein expression of NR4A1, which may be related to its kinase activity. These results suggest that our knowledge of NR4A1 is still very limited and that its paradoxical function may be associated with a different tissue distribution. Further studies are needed to determine whether NR4A1 promotes or inhibits apoptotic activity and whether NR4A1 phosphorylation affects its activity.

Taken together, our findings suggest that AIBP is essential for protecting against acute liver injury. AIBP deficient mice exhibited higher levels of apoptosis and necrosis as well as inflammatory responses upon APAP or CCl4 stimulation, contributing to the poor survival of AIBP-deficient mice after APAP or CCl4 treatment. Aberrant MAPK activation caused by AIBP deficiency caused hepatocyte death, while NR4A1 was necessary and sufficient to alleviate AIBP deficient hepatocyte injury, under APAP stimulation. Thus, our study reveals a role for AIBP in acute liver injury, and provides a molecular explanation for the beneficial effects of the AIBP-MAPK-NR4A1 axis on acute liver injury.

Limitations of the study

In this study, we attempted to elucidate how AIBP inhibits MAPK activation and upregulates NR4A1 expression to protect the liver from drug-induced hepatocyte death. Our results suggest that AIBP can inhibit cell oxidative stress, but AIBP how to play a role in apoptosis and necrosis is not clear.

RESOURCE AVAILABILITY

Lead contact

Further information and requests for resources and reagents should be directed to and will be fulfilled by the lead contact, Cuihua Lu (lch670608@sina.com).

Materials availability

This study did not generate new unique reagents.

Data and code availability

- All data reported in this paper will be shared by the lead contact upon request.
- This paper does not report original code.
- Any additional information required to reanalyze the data reported in this paper is available from the lead contact upon request.

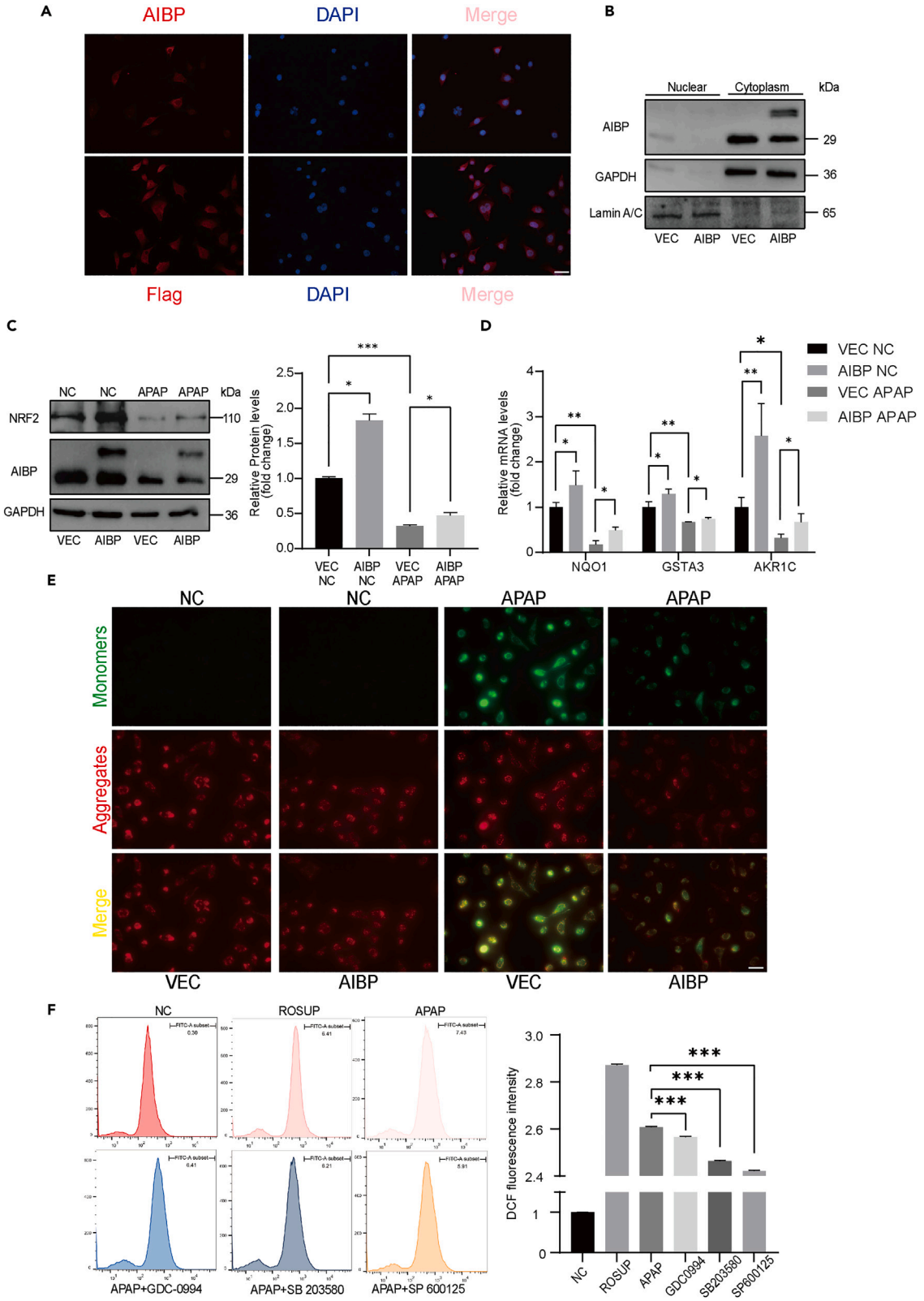
A
AIBP
DAPI
Merge
Flag
DAPI
Merge
B
Nuclear
Cytoplasm
kDa
AIBP
GAPDH
Lamin A/C
29
36
65
VEC
AIBP
VEC
AIBP
C
NC
NC
APAP
APAP
kDa
NRF2
AIBP
GAPDH
110
29
36
VEC
AIBP
VEC
AIBP
Relative Protein levels (fold change)
VEC NC
AIBP NC
VEC APAP
AIBP APAP
D
Relative mRNA levels (fold change)
VEC NC
AIBP NC
VEC APAP
AIBP APAP
NQO1
GSTA3
AKR1C
E
NC
NC
APAP
APAP
Monomers
Aggregates
Merge
VEC
AIBP
VEC
AIBP
F
NC
ROSUP
APAP
APAP+GDC-0994
APAP+SB 203580
APAP+SP 600125
DCF fluorescence intensity
NC
ROSUP
APAP
GDC0994
SB203580
SP600125

Figure 9. AIBP reduces mitochondrial stress and protects mitochondrial function

(A) Overexpression of flag-labeled AIBP protein in 7721 cells, and immunofluorescence detection of AIBP cell localization (Scale bar: 100um).

(B) Control and Flag labeled AIBP proteins were overexpressed in 7721 cells, and nuclear and plasma proteins were isolated to detect the organelle localization of AIBP.

(C) APAP treated HepG2 overexpressed control cell lines and AIBP cell lines, and western blotting detected NRF2 protein expression.

(D) APAP treated HepG2 overexpressed control cell lines and AIBP cell lines, and real-time qPCR was used to analyze the mRNA expression levels of NQO1, GSTA3 and AKR1C.

(E) APAP treated 7721 overexpressed control cell lines and AIBP cell lines, and JC1 reagent was used to detect the mitochondrial membrane potential of the above cells (Scale bar: 20um).

(F) 7721 cells were pretreated with ERK inhibitor GDC-0994, p38 inhibitor SB 203580 and JNK inhibitor SP 600125 for 6 h and then treated with APAP for 24 h. Flow cytometry was used to detect reactive oxygen species production.

ACKNOWLEDGMENTS

This study was supported by the National Natural Science Foundation of China (no. 82070624), Natural Science Foundation of Jiangsu Province (no. BK20210841), Jiangsu Commission of Health (ZDB202006), China Postdoctoral Science Foundation (no.2022M711719), Chinese Foundation for Hepatitis Prevention and Control of the WBN Research Foundation (TQGB20210029), Health Commission of Nantong (QA2021002).

AUTHOR CONTRIBUTIONS

Conceptualization, Y.H.F. and C.H.L.; methodology, Y.H.D., S.J.G., Q.Q.L., and J.C.; investigation, T.M., R.J., Q.Q.R., and Y.H.L.; writing—original draft, T.M. and W.H.; writing—review and editing, Y.H.F. and R.F.M.; funding acquisition, W.H. and C.H.L.; resources, Y.H.F. and R.F.M.; data curation, Y.Y. and S.S.L.; supervision, Y.H.F., R.F.M., and C.H.L.

DECLARATION OF INTERESTS

The authors declare no competing interest.

STAR★METHODS

Detailed methods are provided in the online version of this paper and include the following:

- KEY RESOURCES TABLE
- EXPERIMENTAL MODEL AND STUDY PARTICIPANT DETAILS
  - Patient samples
  - Animal experiments
  - Cell culture and experimental conditions
- METHOD DETAILS
  - Plasmid transfection
  - RNA extraction and real-time PCR
  - Protein extraction and western blotting
  - PI staining of necrotic cells
  - Apoptosis detection
  - Trypan blue staining
  - Cell viability test
  - Reactive oxygen species (ROS) detection
- QUANTIFICATION AND STATISTICAL ANALYSIS
  - Statistical analysis

SUPPLEMENTAL INFORMATION

Supplemental information can be found online at https://doi.org/10.1016/j.isci.2024.110873.

Received: November 11, 2023
Revised: April 30, 2024
Accepted: August 30, 2024
Published: September 12, 2024

REFERENCES

1. Fontana, R.J., Seeff, L.B., Andrade, R.J., Björnsson, E., Day, C.P., Serrano, J., and Hoofnagle, J.H. (2010). Standardization of Nomenclature and Causality Assessment in Drug-Induced Liver Injury: Summary of a Clinical Research Workshop. Hepatology *52*, 730–742.
2. Hassan, A., and Fontana, R.J. (2019). The diagnosis and management of idiosyncratic drug-induced liver injury. Liver International *39*, 31–41.
3. Gu, X., and Manautou, J.E. (2012). Molecular mechanisms underlying chemical liver injury. Expet Rev. Mol. Med. *14*, e4.
4. McGill, M.R., and Jaeschke, H. (2019). Animal models of drug-induced liver injury. Biochim Biophys Acta Mol Basis Dis. *1865*, 1031–1039.
5. Larson, A.M., Polson, J., Fontana, R.J., Davern, T.J., Lalani, E., Hynan, L.S., Reisch, J.S., Schiødt, F.V., Ostapowicz, G., Shakil, A.O., and Lee, W.M. (2005). Acetaminophen-induced acute liver failure: results of a United States multicenter, prospective study. Hepatology *42*, 1364–1372.
6. Lee, S.S., Buters, J.T., Pineau, T., Fernandez-Salguero, P., and Gonzalez, F.J. (1996). Role of CYP2E1 in the Hepatotoxicity of Acetaminophen. Journal of Biological Chemistry *271*, 12063–12067.
7. Jaeschke, H., Knight, T.R., and Bajt, M.L. (2003). The role of oxidant stress and reactive nitrogen species in acetaminophen hepatotoxicity. Toxicol. Lett. *144*, 279–288.

8. McGill, M.R., Sharpe, M.R., Williams, C.D., Taha, M., Curry, S.C., and Jaeschke, H. (2012). The mechanism underlying acetaminophen-induced hepatotoxicity in humans and mice involves mitochondrial damage and nuclear DNA fragmentation. J. Clin. Investig. *122*, 1574–1583.
9. Choi, S.H., Wallace, A.M., Schneider, D.A., Burg, E., Kim, J., Alekseeva, E., Ubags, N.D., Cool, C.D., Fang, L., Suratt, B.T., and Miller, Y.I. (2018). AIBP augments cholesterol efflux from alveolar macrophages to surfactant and reduces acute lung. Inflammation *3*, 120519.
10. Westerterp, M. (2018). AIBP decreases atherogenesis by augmenting cholesterol efflux. Atherosclerosis *273*, 117–118.
11. Zhang, M., Zhao, G.J., Yao, F., Xia, X.D., Gong, D., Zhao, Z.W., Chen, L.Y., Zheng, X.L., Tang, X.E., and Tang, C.K. (2018). AIBP Reduces Atherosclerosis by Promoting Reverse Cholesterol Transport and Ameliorating Inflammation in apoE(-/-) Mice. Atherosclerosis *273*, 122–130.
12. Fang, L., Liu, C., and Miller, Y.I. (2014). Zebrafish models of dyslipidemia: relevance to atherosclerosis and angiogenesis. Transl. Res. *163*, 99–108.
13. Fang, L., Choi, S.H., Baek, J.S., Liu, C., Almazan, F., Ulrich, F., Wiesner, P., Taleb, A., Deer, E., Pattison, J., et al. (2013). Control of angiogenesis by AIBP-mediated cholesterol efflux. Nature *498*, 118–122.
14. Zhang, M., Li, L., Xie, W., Wu, J.F., Yao, F., Tan, Y.L., Xia, X.D., Liu, X.Y., Liu, D., Lan, G., et al. (2016). Apolipoprotein A-1 binding protein promotes macrophage cholesterol efflux by facilitating apolipoprotein A-1 binding to ABCA1 and preventing ABCA1 degradation. Atherosclerosis *248*, 149–159.
15. Marbaix, A.Y., Tyteca, D., Niehaus, T.D., Hanson, A.D., Linster, C.L., and Van Schaftingen, E. (2014). Occurrence and subcellular distribution of the NADPHX repair system in mammals. Biochem. J. *460*, 49–58.
16. Sorci-Thomas, M.G., and Thomas, M.J. (2017). AIBP, NAXE, and Angiogenesis: What's in a Name? Circ. Res. *120*, 1690–1691.
17. Marbaix, A.Y., Noël, G., Detroux, A.M., Vertommen, D., Van Schaftingen, E., and Linster, C.L. (2011). Extremely Conserved ATP- or ADP-dependent Enzymatic System for Nicotinamide Nucleotide Repair. Journal of Biological Chemistry *286*, 41246–41252.
18. Mao, R., Meng, S., Gu, Q., Araujo-Gutierrez, R., Kumar, S., Yan, Q., Almazan, F., Youker, K.A., Fu, Y., Pownall, H.J., and Cooke, J.P. (2017). AIBP Limits Angiogenesis Through gamma-Secretase-Mediated Upregulation of Notch Signaling. Circ. Res. *120*, 1727–1739.
19. Mayneris-Perxachs, J., Puig, J., Burcelin, R., Dumas, M.E., Barton, R.H., Hoyles, L., Federici, M., and Fernández-Real, J.M. (2020). The APOA1bp-SREBF-NOTCH axis is associated with reduced atherosclerosis risk in morbidly obese patients. Clinical Nutrition *39*, 3408–3418.
20. Zhang, M., Zhao, G.J., Yin, K., Xia, X.D., Gong, D., Zhao, Z.W., Chen, L.Y., Zheng, X.L., Tang, X.E., and Tang, C.K. (2018). Apolipoprotein A-1 Binding Protein Inhibits Inflammatory Signaling Pathways by Binding to Apolipoprotein A-1 in THP-1 Macrophages. Circ. J. *82*, 1396–1404.
21. Fang, L., and Miller, Y.I. (2019). Regulation of lipid rafts, angiogenesis and inflammation by AIBP. Curr. Opin. Lipidol. *30*, 218–223.
22. Choi, S.H., Agatisa-Boyle, C., Gonen, A., Kim, A., Kim, J., Alekseeva, E., Tsimikas, S., and Miller, Y.I. (2021). Intracellular AIBP (Apolipoprotein A-I Binding Protein) Regulates Oxidized LDL (Low-Density Lipoprotein)-Induced Mitophagy in Macrophages. Arterioscler. Thromb. Vasc. Biol. *41*, e82–e96.
23. Jackson, A.O., Rahman, G.A., and Long, S. (2021). Apolipoprotein-AI and AIBP Synergetic Anti-inflammation as Vascular Diseases Therapy: The New perspective. Molecular and Cellular Biochemistry *4768*, 3065–3078.
24. Fang, J.Y., and Richardson, B.C. (2005). The MAPK signalling pathways and colorectal cancer. Lancet Oncol. *6*, 322–327.
25. Zhang, J., Min, R.W., Le, K., Zhou, S., Aghajan, M., Than, T.A., Win, S., and Kaplowitz, N. (2017). The Role of MAP2 Kinases and P38 Kinase in Acute Murine Liver Injury Models. Cell Death & Disease *86*, e2903.
26. Wu, L., and Chen, L. (2018). Characteristics of Nur77 and its ligands as potential anticancer compounds. Mol. Med. Rep. *18*, 4793–4801.
27. Safe, S., and Karki, K. (2021). The paradoxical roles of orphan nuclear receptor 4a (nr4a) in cancer. Mol. Cancer Res. *19*, 180–191.
28. Kolluri, S.K., Bruey-Sedano, N., Cao, X., Lin, B., Lin, F., Han, Y.H., Dawson, M.I., and Zhang, X.K. (2003). Mitogenic Effect of Orphan Receptor TR3 and its Regulation by MEKK1 in Lung Cancer cells. Molecular and cellular biology *2323*, 8651–8667.
29. Lee, S.O., Andey, T., Jin, U.H., Kim, K., Singh, M., and Safe, S. (2012). The nuclear receptor TR3 regulates mTORC1 signaling in lung cancer cells expressing wild-type p53. Oncogene *31*, 3265–3276.
30. Wohlkoenig, C., Leithner, K., Olschewski, A., Olschewski, H., and Hrzenjak, A. (2017). TR3 is involved in hypoxia-induced apoptosis resistance in lung cancer cells downstream of HIF-1α. Lung Cancer *111*, 15–22.
31. Pu, Z.Q., Liu, D., Lobo Mouguegue, H.P.P., Jin, C., Sadiq, E., Qin, D., Yu, T., Zong, C., Chen, J., Zhao, R., et al. (2020). NR4A1 counteracts JNK activation incurred by ER stress or ROS in pancreatic beta-cells for protection. J. Cell Mol. Med. *24*, 14171–14183.
32. Hu, Y., Zhan, Q., Liu, H.X., Chau, T., Li, Y., and Wan, Y.J.Y. (2014). Accelerated Partial Hepatectomy-Induced Liver Cell Proliferation Is Associated with Liver Injury in Nur77 Knockout Mice. The American journal of pathology *184*, 3272–3283.
33. He, L., Yuan, L., Yu, W., Sun, Y., Jiang, D., Wang, X., Feng, X., Wang, Z., Xu, J., Yang, R., and Zhang, W. (2020). A Regulation Loop between YAP and NR4A1 Balances Cell Proliferation and Apoptosis. Cell reports *33*.
34. Chen, Y., Liu, K., Zhang, J., Hai, Y., Wang, P., Wang, H., Liu, Q., Wong, C.C.L., Yao, J., Gao, Y., et al. (2020). c-Jun NH(2) -Terminal Protein Kinase Phosphorylates the Nrf2-ECH Homology 6 Domain of Nuclear Factor Erythroid 2-Related Factor 2 and Downregulates Cytoprotective Genes in Acetaminophen-Induced Liver Injury in Mice. Hepatology *71*, 1787–1801.
35. Sun, Y., Li, T.Y., Song, L., Zhang, C., Li, J., Lin, Z.Z., Lin, S.C., and Lin, S.Y. (2018). Liver-specific Deficiency of Unc-51 like Kinase 1 and 2 Protects Mice from Acetaminophen-Induced Liver Injury. Hepatology *676*, 2397–2413.
36. Zhao, S., Song, T., Gu, Y., Zhang, Y., Cao, S., Miao, Q., Zhang, X., Chen, H., Gao, Y., Zhang, L., et al. (2021). Hydrogen Sulfide Alleviates Liver Injury Through the S-Sulfhydrated-Kelch-Like ECH-Associated Protein 1/Nuclear Erythroid 2-Related Factor 2/Low-Density Lipoprotein Receptor-Related Protein 1 Pathway. Hepatology *73*, 282–302.
37. Ghanim, B.Y., and Qinna, N.A. (2022). Nrf2/ARE axis signalling in hepatocyte cellular death. Mol. Biol. Rep. *49*, 4039–4053.
38. Xu, Q., Deng, Y., Ming, J., Luo, Z., Chen, X., Chen, T., Wang, Y., Yan, S., Zhou, J., Mao, L., and Sun, W. (2022). Methyl 6-O-Cinnamoyl-Alpha-D-Glucopyranoside Ameliorates Acute Liver Injury by Inhibiting Oxidative Stress through the Activation of Nrf2 Signaling Pathway. Frontiers in Pharmacology *13*, 873938.
39. Watkins, P.B., and Seeff, L.B. (2006). Drug-induced liver injury: summary of a single topic clinical research conference. Hepatology *43*, 618–631.
40. Thawley, V. (2017). Acute Liver Injury and Failure. Veterinary Clinics: Small Animal Practice *47*, 617–630.
41. Chen, D., Ni, H.M., Wang, L., Ma, X., Yu, J., Ding, W.X., and Zhang, L. (2019). p53 Up-regulated Modulator of Apoptosis Induction Mediates Acetaminophen-Induced Necrosis and Liver Injury in Mice. Hepatology *69*, 2164–2179.
42. Hanawa, N., Shinohara, M., Saberi, B., Gaarde, W.A., Han, D., and Kaplowitz, N. (2008). Role of JNK translocation to mitochondria leading to inhibition of mitochondria bioenergetics in acetaminophen-induced liver injury. J. Biol. Chem. *283*, 13565–13577.
43. Liu, X., Wang, Y., Lu, H., Li, J., Yan, X., Xiao, M., Hao, J., Alekseev, A., Khong, H., Chen, T., and Huang, R. (2019). Genome-wide Analysis Identifies NR4A1 as a Key Mediator of T Cell Dysfunction. Nature *567*, 525–529.
44. Palumbo-Zerr, K., Zerr, P., Distler, A., Fliehr, J., Mancuso, R., Huang, J., Mielenz, D., Tomcik, M., Fürnrohr, B.G., Scholtysek, C., and Dees, C. (2015). Orphan Nuclear Receptor NR4A1 Regulates Transforming Growth Factor-Beta Signaling and Fibrosis. Nature medicine *21*, 150–158.
45. Godoi, P.H., Wilkie-Grantham, R.P., Hishiki, A., Sano, R., Matsuzawa, Y., Yanagi, H., Munte, C.E., Chen, Y., Yao, Y., Marassi, F.M., and Kalbitzer, H.R. (2016). Orphan Nuclear Receptor NR4A1 Binds a Novel Protein Interaction Site on Anti-apoptotic B Cell Lymphoma Gene 2 Family Proteins. Journal of Biological Chemistry *291*, 14072–14084.
46. Yang, H.X., Sun, J.H., Yao, T.T., Li, Y., Xu, G.R., Zhang, C., Liu, X.C., Zhou, W.W., Song, Q.H., Zhang, Y., and Li, A.Y. (2021). Bellidifolin ameliorates isoprenaline-induced myocardial fibrosis by regulating tgf-beta1/smads and p38 signaling and preventing nr4a1 cytoplasmic localization. Front. Pharmacol. *12*, 644886.
47. Chen, H.Z., Zhao, B.X., Zhao, W.X., Li, L., Zhang, B., and Wu, Q. (2008). Akt Phosphorylates the TR3 Orphan Receptor and Blocks its Targeting to the Mitochondria. Carcinogenesis *29*, 2078–2088.

STAR★METHODS

KEY RESOURCES TABLE

REAGENT or RESOURCE	SOURCE	IDENTIFIER
Antibodies		
GAPDH Monoclonal antibody	proteintech	Cat# 60004-1-Ig, RRID:AB_2107436
APOA1BP Antibody	Novus	Cat# NBP1-55934-0.1mg, RRID:AB_11017202
Bax Antibody	Santa Cruz	Cat# sc-7480, RRID:AB_626729
Caspase3 Antibody	Cell Signaling Technology	Cat# 9662, RRID:AB_331439
Cleaved-Caspase3 Antibody	Abcam	Cat# ab32042, RRID:AB_725947
RIP3 Polyclonal antibody	proteintech	Cat# 17563-1-AP, RRID:AB_2178659
Phospho-MLKL (Ser345) (D6E3G) Rabbit mAb	Cell Signaling Technology	Cat# 37333, RRID:AB_2799112
MLKL Monoclonal antibody	proteintech	Cat# 66675-1-Ig, RRID:AB_2882029
NR4A1 Polyclonal antibody	proteintech	Cat# 25851-1-AP, RRID:AB_2880269
Phospho-p44/42 MAPK (Erk1/2) (Thr202/ Tyr204) (D13.14.4E) XP® Rabbit mAb	Cell Signaling Technology	Cat# 4370, RRID:AB_2315112
p44/42 MAPK (Erk1/2) (137F5) Rabbit mAb	Cell Signaling Technology	Cat# 4695, RRID:AB_390779
Phospho-p38 MAPK (Thr180/Tyr182) (28B10) Mouse mAb	Cell Signaling Technology	(Cat# 9216, RRID:AB_331296
p38 MAPK (D13E1) XP® Rabbit mAb	Cell Signaling Technology	Cat# 8690, RRID:AB_10999090
Phospho-JNK (Tyr185) Recombinant antibody	proteintech	Cat# 80024-1-RR, RRID:AB_2882943
Anti- JNK1+JNK2+JNK3 Rabbit pAb	Servicebio	GB114321-100
Lamin A/C Antibody	Santa Cruz	(Cat# sc-376248, RRID:AB_10991536
NRF2, NFE2L2 Recombinant antibody	proteintech	Cat# 80593-1-RR, RRID:AB_2918904
Chemicals, peptides, and recombinant proteins		
GDC 0994	MedChemExpress	HY-15947
SB 203580	MedChemExpress	HY-10256
SP 600125	MedChemExpress	HY-12041
APAP	Sangon Biotech	A506808
Experimental models: Cell lines		
SMMC7721	BeNa Culture Collection	BNCC338089
HepG2	BeNa Culture Collection	BNCC338070
Software and algorithms		
ImageJ	ImageJ Software	https://imagej.net/
Graphpad Prism 9	GraphPad Software	https://www.graphpad.com/
Image Lab	Image Lab Software	https://www.bio-rad.com/

EXPERIMENTAL MODEL AND STUDY PARTICIPANT DETAILS

Patient samples

Serum samples were collected from the Affiliated Hospital of Nantong University. The collection of samples was approved by the ethics committee of the Affiliated Hospital of Nantong University and complied with the principles outlined in the Helsinki Declaration. All samples were collected with the informed consent of the participants, and no compensation was provided to any participant. The samples included 60 patients with acute liver injury and 101 patients undergoing general physical examination.

Animal experiments

Wild-type (WT) mice were purchased from the Experimental Animal Center of Nantong Medical University. *AIBP* knockout (KO)(Naxe$^{-/-}$) mice were provided by Dr. Fan and were generated from heterozygous intercrosses. All strains were maintained on a C57BL/6 background.

8-week-old Male mice were randomly assigned to the different treatment groups. Animal were fasted overnight, but allowed access to water, prior to experiments.

APAP (Sangon Biotech, A506808) was dissolved in warm phosphate-buffered saline (PBS, 55°C) and cooled to 37°C before injection. The dose of APAP chosen in this study was the same as those used in previous studies.[41] The blood and liver tissue were collected at 6 h, 12 h and 24 h after the APAP exposure.

A 1:1 mixture of CCl4 (carbon tetrachloride) and olive oil was used to obtain 50% of experimental CCl4. Wild-type and AIBP$^{-/-}$ mice were randomly divided into groups to induce acute liver injury by intraperitoneal injection of 50% CCl4 at 5 μL/g. Follow-up treatment was similar to above.

The item was conducted according to animal use and feeding standards established by the Committee of the China Animal Protection Association.

Cell culture and experimental conditions

Hepatocellular carcinoma HepG2, SMMC-7721 and human normal hepatocellular carcinoma HL-7002 (LO2) were kindly provided by BeNa Culture Collection (BNCC, China). The cells were cultured with 10% fetal bovine serum (FBS, gibico, Australia), 1% penicillin-strep-tomycin (NCM Biotech, China), and 10 μg/mL tetracycline hydrochloride(Sangong Biotech, China) in complete Dulbecco's modified Eagle's medium (DMEM, HyClone, USA) in an incubator containing 5% CO2 at 37°C.

Cells for experiment were previously implanted in six-well plates. When the cells grew to 70% density, 4 mM CCl4 dissolved in DMSO (dimethyl sulfoxide) and 10 mM APAP dissolved in PBS were added into the medium separately.

METHOD DETAILS

Plasmid transfection

Cells for transfection were previously implanted in six-well plates. When the cells grew to 70% density, the medium was changed to serum-free basal medium DMEM and transfected with Lipofectamine 2000 transfection reagent (Invitrogen, USA). Six h after transfection, DMEM was replaced with DMEM complete medium containing only 10%FBS, and cells were screened 48 h later with purinomycin (Apexbio, USA) or G418 sulfate (Sangong Biotech, China) according to their resistant genes.

sgRNA sequences used:
NAXE-sgRNA-1: CCGAGCGACAGGCGATGGTC,
NAXE-sgRNA-2: CCAGACCATCGCCTGTCGCT,
NAXE-sgRNA-3: TAAGTTGGTCCACGCTGAAC,
NAXE-sgRNA-4: CGTGGACCAACTTATGGAAC,
Vector: LentiCRISPRv2-puro.
NAXE-sgRNA-3 was used to knock down the expression of AIBP.

RNA extraction and real-time PCR

Total RNA was extracted from liver tissues and cells with TRIZOL reagent (Vazyme, China), and RNA content was detected by Nanodrop 8000 (ND, Thermo Fisher Scientific, USA). The cDNA synthesis kit (Vazyme, China) was used for RNA reverse transcription, followed by RT-qPCR using the SYBER GREEN kit (Vazyme, China). 18s was used as an internal reference to mRNA. All the primers were synthesized by Shanghai Sangong Biological Company (Sangong Biotech, China), and the primers sequence were shown as follow:

18s:GGGGATTGGTTTTGACGTTTTTGCG, AAGCATTAAATAAAGCGAATACATCCTTAT.
Naxe: ATTCCACAGCATCCTGAGTGTCTTG, GTGCCGTCAGTGAGATGAGTAAGTC.
NAXE: AGCGTGGACCAACTTATGGAACTG, AGCACAGACCAGACCATCTCCTC.
NR4A1: AAAATCCCTGGCTTCATTGAG, TTTAGATCGGTATGCCAGGCG.
NQO1: TCACCGAGAGCCTAGTTCC, TCATGGCATAGTTGAAGGAACG.
GSTA3: TCGACGGGATGAAACTGGTG, CAGATCCGCCACTCCTTCTG.
AKR1C: CATGCCTGTCCTGGGATTT, AGAATCAATATGGCGGAAGC.

Protein extraction and western blotting

Liver tissues and cells were lysed with RIPA lysis buffer (Beyotime, China) containing 1%phosphatase inhibitors (PhosSTOP, Roche Diagnostics GmbH, Germany) and 2%protease inhibitor (cOmplete, Roche Diagnostics GmbH, Germany). The lysate was centrifuged at 12000 rpm at 4°C for 10 min and the supernatant was collected. Protein samples were obtained by adding 5x loading buffer (Beyotime, China), mixing and boiling at 100°C for 5 min. The protein was separated by SDS-PAGE and electrically transferred to PVDF membrane (Roche Diagnostics GmbH, Germany). TBST containing 5% skim milk was then used to block the membrane at room temperature for 2h, and TBS to wash for 5min. The diluted primary antibody was incubated overnight. After three times of TBST washing for 10min, the specific secondary antibody was incubated for 2h at room temperature. After three times of TBST washing, the bands were observed with an enhanced chemiluminescent kit (NCM Biotech, China) by bioimaging system (Bio-Rad, USA). GAPDH was used as a protein internal reference, and the protein bands were quantified using ImageJ.

Used antibody

GAPDH(1:5000; proteintech, 60004-1-Ig), AIBP(1:1000; Novus, NBP2-30626), Bax(1:500; Santa Cruz, sc-7480), Caspase3(1:1000; Cell Signaling Technology, #9662), Cleaved-Caspase3(1:500; Abcam, ab32042), RIP3(1:1000; proteintech, 17563-1-AP), P-MLKL(1:1000; Cell Signaling Technology, #37333), MLKL(1:5000; proteintech, 66675-1-Ig), NR4A1(1:1000; proteintech, 25851-1-AP), P-ERK(1:1000; Cell Signaling Technology, #4370), ERK(1:1000; Cell Signaling Technology, #4695), P-p38(1:1000; Cell Signaling Technology, #9216), p38(1:1000; Cell Signaling Technology, #8690), P-JNK(1:1000; proteintech, 80024-1-RR), JNK(1:1000; Servicebio, GB114321-100), Lamin A/C(1:500; Santa Cruz, sc-376248), NRF2(1:1000; proteintech, 80593-1-RR).

PI staining of necrotic cells

Propyl iodide (PI, Beyotime, China) can penetrate the damaged cell membranes of dead cells and release red fluorescence after embedding double-stranded DNA. After the induced cell injury, the cells were gently cleaned with PBS and readded with 1 μg/ml propidium iodide in cell culture solution. The cells were incubated at 37°C without light for 30 min, and were gently cleaned with PBS and observed with fluorescence microscope. Hoechst 33342 (Beyotime, China) as a live cell control.

Apoptosis detection

The cell samples were collected for preparation of single-cell suspension, which was added with 5ul Annexin V-FITC and 10ul propidium iodide staining solution. After mixing, the cells were incubated at room temperature and protected from light for 20 min. The cells were suspended every 5 min for full staining. Using FlowJo-10.6.2 quantitative results, Annexin V-positive cells were defined as early apoptotic cells and Annexin V-PI double-positive cells were defined as late apoptotic or necrotic cells.

Trypan blue staining

Trypan Blue (RWD, China) can penetrate the cell membrane of dead cells and stain them blue, while living cells are colorless and transparent. The cell samples to be tested were prepared as single-cell suspension, which was evenly mixed with 0.4% Trypan Blue solution at 1:1 and added into the cell counting plate (RWD, China). An automatic cell counter (C100, RWD, China) observed cell components and counted the proportion of dead cells and alive cells.

Cell viability test

Cell count kit 8 (CCK8, hanbio, China) measured cell viability. Cells were treated with different doses of APAP for 24 h and incubated with 10% CCK8 reagent for 2 h. Then, Thermo Fisher Scientific (Thermo, USA), the absorbance value was measured at 510 nm to calculate cell viability.

Reactive oxygen species (ROS) detection

The DCFH-DA probe was diluted with DMEM at 1:1000 (Beyotime, China), and the sample cells were collected and suspended in the diluted DCFH-DA probe solution and incubated in an incubator at 37°C for 20 min. Invert and mix every 5 min to make full contact between the probe and the cells. The cells were washed with DMEM three times to remove the DCFH-DA that did not enter the cells. After PBS was suspended, flow cytometry (FACSCalibur, BD, USA) detected fluorescence signals at 488nm excitation wavelength and 525nm emission wavelength. Quantitative experiment results were obtained using FlowJo-10.6.2.

QUANTIFICATION AND STATISTICAL ANALYSIS

Statistical analysis

Statistical analysis was performed using GraphPad Prism software (version 9.0, GraphPad). All measurements are reported as mean ± standard error of the mean (SEM). Statistical analysis involved the utilization of either the Student's t test or one-way analysis of variance (ANOVA). Statistical significance was defined as p values < 0.05.